

# $\alpha$ V-Integrins Are Required for Mechanotransduction in MDCK Epithelial Cells

Terhi P. Teräväinen<sup>1</sup>, Satu M. Myllymäki<sup>1</sup>, Jens Friedrichs<sup>2,4</sup>, Nico Strohmeyer<sup>3</sup>, Jose V. Moyano<sup>6</sup>, Chuanyue Wu<sup>5</sup>, Karl S. Matlin<sup>6</sup>, Daniel J. Muller<sup>3</sup>, Aki Manninen<sup>1\*</sup>

**1** Biocenter Oulu, Oulu Center for Cell-Matrix Research, Department of Medical Biochemistry and Molecular Biology, University of Oulu, Oulu, Finland, **2** Leibniz Institute of Polymer Research Dresden, Institute of Biofunctional Polymer Materials, Dresden, Germany, **3** ETH Zürich, Department of Biosystems Science and Engineering, Basel, Switzerland, **4** Biotechnology Center, Dresden University of Technology, Dresden, Germany, **5** Department of Pathology, University of Pittsburgh School of Medicine, Pittsburgh, Pennsylvania, United States of America, **6** Department of Surgery, Committee on Cell Physiology, and Committee on Molecular Pathogenesis and Molecular Medicine, The University of Chicago, Chicago, Illinois, United States of America

## Abstract

The properties of epithelial cells within tissues are regulated by their immediate microenvironment, which consists of neighboring cells and the extracellular matrix (ECM). Integrin heterodimers orchestrate dynamic assembly and disassembly of cell-ECM connections and thereby convey biochemical and mechanical information from the ECM into cells. However, the specific contributions and functional hierarchy between different integrin heterodimers in the regulation of focal adhesion dynamics in epithelial cells are incompletely understood. Here, we have studied the functions of RGD-binding  $\alpha$ V-integrins in a Madin Darby Canine Kidney (MDCK) cell model and found that  $\alpha$ V-integrins regulate the maturation of focal adhesions (FAs) and cell spreading.  $\alpha$ V-integrin-deficient MDCK cells bound collagen I (Col I) substrate via  $\alpha$ 2 $\beta$ 1-integrins but failed to efficiently recruit FA components such as talin, focal adhesion kinase (FAK), vinculin and integrin-linked kinase (ILK). The apparent inability to mature  $\alpha$ 2 $\beta$ 1-integrin-mediated FAs and link them to cellular actin cytoskeleton led to disrupted mechanotransduction in  $\alpha$ V-integrin deficient cells seeded onto Col I substrate.

**Citation:** Teräväinen TP, Myllymäki SM, Friedrichs J, Strohmeyer N, Moyano JV, et al. (2013)  $\alpha$ V-Integrins Are Required for Mechanotransduction in MDCK Epithelial Cells. PLoS ONE 8(8): e71485. doi:10.1371/journal.pone.0071485

**Editor:** Adam J. Engler, University of California, San Diego, United States of America

**Received:** February 6, 2013; **Accepted:** June 29, 2013; **Published:** August 19, 2013

**Copyright:** © 2013 Teräväinen et al. This is an open-access article distributed under the terms of the Creative Commons Attribution License, which permits unrestricted use, distribution, and reproduction in any medium, provided the original author and source are credited.

**Funding:** This work was supported by Academy of Finland Grants (114330, 135560 and 140974), by Federal Ministry of Education and Research, Germany, by Biocenter Finland, and by the Sigrid Juselius Foundation. The funders had no role in study design, data collection and analysis, decision to publish, or preparation of the manuscript.

**Competing Interests:** The authors have declared that no competing interests exist.

\* E-mail: aki.manninen@oulu.fi

## Introduction

The immediate cellular microenvironment, including the surrounding ECM, regulates cellular properties in different locations within tissues. Dynamic regulation of epithelial cell differentiation is crucial for tissue development and function. Epithelial cells are commonly underlined by a special type of ECM, the basement membrane (BM), which consists of laminins, collagen IV and various proteoglycans. In addition to the biochemical diversity of the ECM and its embedded signals (such as ECM-bound growth factors), mechanical properties of the ECM have a major influence on cellular responses [1–3]. Whereas laminin establishes a basal cue to guide apico-basal cell polarization [2,4–7] the mechanical properties of the ECM are largely dependent upon fibrillar collagen and fibronectin (FN) networks. Interactions between epithelial cells and the ECM play an important role in the regulation of proliferation, survival and migration of normal and carcinoma cells [8,9].

Dynamic assembly and disassembly of integrin-mediated focal adhesions is crucial for epithelial cell migration, mechanotransduction and epithelial morphogenesis. Integrins are heterodimeric cellular receptors for laminins, collagens and FN and have been reported to actively participate to the hierarchical co-assembly of these interconnected networks [10–14]. Integrins are also crucial components of the tension-sensing machinery that detects the

mechanical properties of the ECM [2,15]. Most cells express many different integrin heterodimers that interact with partially overlapping repertoires of ECM molecules. A complex signaling cross-talk operates between the different integrin species [16–19]. While  $\beta$ 1- and  $\beta$ 4-integrins appear to mediate collagen adhesion and the laminin-based basal cue guiding epithelial cell polarity [5,6,20], the functional roles of a promiscuous group of RGD-motif binding integrins in epithelial cells are less clear. RGD-motifs are abundant in both ECM proteins and soluble factors [21]. In fibroblasts adhering to FN,  $\alpha$ V- and  $\beta$ 1-integrins cooperate to form focal adhesions [2,15]. However, the specific role of RGD-binding  $\alpha$ V-integrins in epithelial cell adhesion or their possible functional interplay with  $\beta$ 1-integrins is not thoroughly understood.

Here, we have studied the functional roles of RGD-binding integrins expressed in epithelial Madin Darby Canine Kidney (MDCK) cells and their possible crosstalk with  $\beta$ 1-integrin-dependent functions. Interestingly,  $\alpha$ V-integrins were found to regulate cell spreading not only on FN but also on other ECM substrates such as collagen I (Col I) and LN-511 to which adhesion was mediated by  $\beta$ 1-integrins. The surface exposure or initial binding of  $\alpha$ 2 $\beta$ 1-integrins (the main collagen receptor in MDCK cells) to Col I was not affected in  $\alpha$ V-integrin knockdown (Itg $\alpha$ V-KD) MDCK cells, but the recruitment of talin and multiple other components of focal adhesions (FAs) was abrogated resulting in

perturbed mechanosensory responses. Whereas inhibition of talin-1, FAK or ILK expression led to impaired cell spreading only depletion of talin-1 replicated the defect in cellular mechanotransduction seen in Itg $\alpha$ V-KD cells. These findings identify a novel role for  $\alpha$ V-integrins in modulating talin-dependent mechanotransduction in epithelial MDCK cells.

## Results

### Characterization of the functional roles of RGD-binding integrins in MDCK cells

To study the functions of RGD-binding integrins in epithelial cells we analyzed the integrin mRNA expression profile in non-transformed MDCK cells by quantitative PCR. Out of the RGD-interacting integrin subunits, MDCK cells expressed  $\beta$ 1-,  $\beta$ 3-,  $\beta$ 5-,  $\beta$ 6-,  $\beta$ 8-,  $\alpha$ 5- and  $\alpha$ V-integrins (data not shown, see also [6]). To study the functional roles of these integrin subunits, we depleted their expression in MDCK cells using RNA interference (RNAi). Efficient depletion of the target mRNAs was confirmed using qPCR (**Table S1A**). The depletion of the different integrins at protein level was analyzed using western blotting and metabolic labeling experiments (**Fig. S1**).

FN can serve as a ligand for all of the above-mentioned integrins [22]. Moreover,  $\alpha$ 5 $\beta$ 1- and  $\alpha$ V $\beta$ 3-integrins are also central for the assembly of FN matrices in some cell types [23]. Adhesive properties of the different Itg-KD cells on FN were analyzed employing a cell washing assay [24]. These data indicated that  $\alpha$ V $\beta$ 6-integrin is the main adhesion receptor for FN in MDCK cells (**Fig. S2A**).  $\beta$ 1-integrins were crucial for efficient adhesion to collagen I (Col I), laminin-511 (LN-511) and basement membrane extract (BME) but they were dispensable for FN adhesion (**Fig. S2**, see also [6]). Surprisingly, in addition to Itg $\beta$ 1-KD cells, a notable proportion of Itg $\alpha$ V-KD cells detached during washing steps from Col I-, LN-511- and BME-coated wells (**Fig. S2B–D**).

Our earlier data implicated  $\alpha$ 2 $\beta$ 1-integrin as an important Col I receptor in MDCK cells [6]. However, because laminins and collagens also have RGD domains [25–28], we next tested whether  $\alpha$ V-integrins might directly interact with Col I. The cell washing assay provides only semi-quantitative data about relative resistance of cells to shear forces during washing steps. To quantitatively compare the adhesion forces of control and Itg $\alpha$ V-KD cells to Col I substrate, an atomic force microscopy (AFM)-based single cell force spectroscopy (SCFS) assay was employed [29,30]. We found that initial adhesion strengths of control and Itg $\alpha$ V-KD cells to Col I were similar (**Fig. 1A**). SCFS-measurements confirmed that Itg $\alpha$ 2-KD cells have very poor Col I binding capacity indicating that adhesion to Col I is mediated via  $\alpha$ 2 $\beta$ 1-integrins (**Fig. 1B**). Therefore, it is unlikely that  $\alpha$ V-integrins directly contribute to Col I binding. Analysis of membrane tethers (see **Fig. S3A**), formed upon separating control and Itg $\alpha$ V-KD cells from Col I substrate, did not reveal significant differences in the tether rupture force (**Fig. 1C**) or in the number or length of tethers (**Fig. 1D**). As the tether rupture force and the length of membrane tethers depend both on the membrane properties and lifetime of receptor-ligand bonds [31] it can be also assumed that the availability of  $\alpha$ 2 $\beta$ 1-integrins at the cell surface, their affinity to Col I and the membrane-cortex interactions were similar in control and Itg $\alpha$ V-KD cells.

Given the important role of  $\alpha$ 2 $\beta$ 1-integrin in adhesion to collagen the availability of  $\alpha$ 2 $\beta$ 1-integrins at the cell surface was also confirmed by a surface biotinylation assay. The surface biotinylation assay did not reveal significant differences in the surface exposure of  $\alpha$ 2- or  $\beta$ 1-integrin subunits (**Fig. 1E–F**).

Moreover, metabolic labeling experiments showed that the steady-state expression levels and the composition of  $\beta$ 1-integrin heterodimers were similar in control and in Itg $\alpha$ V-KD cells where  $\alpha$ V-integrin protein levels were undetectable (**Fig. S1G**). Incubation of MDCK cells with short RGD-motif containing polypeptides efficiently inhibited FN adhesion but did not perturb adhesion to LN-511 or Col I (unpublished observations, see also [24,32,33]). Finally, in MDCK cells seeded onto FN,  $\alpha$ V-integrin-red fluorescent protein (RFP) fusion protein accumulated to pericellular foci whereas no such foci were seen on Col I substrate where relatively uniform membrane staining was observed (**Fig. S1H**). Thus, we conclude that  $\alpha$ V-integrins do not play a significant role as collagen binding receptors in MDCK cells which instead adhere to collagen mainly via  $\alpha$ 2 $\beta$ 1-integrins.

### $\alpha$ V-integrins regulate cell spreading on collagen I and laminin-511 matrices

The functional regulation of integrins underlies cell spreading dynamics that involves coordinated assembly and disassembly of integrin-mediated cell-matrix contacts, linkage of these contact sites to the cellular cytoskeleton leading to cell spreading coordinated by the actin network dynamics [34]. Itg $\alpha$ V-KD cells did not adhere to FN and only few poorly spread Itg $\alpha$ V-KD cells could be recovered on this substrate (**Fig. 2A**). In line with the observed FN adhesion defect, Itg $\beta$ 6-KD cells spread poorly on this substrate (**Fig. 2A**). Itg $\beta$ 3-KD cells displayed a significant spreading defect on FN suggesting that it also contributes to the regulation of cellular response upon adhesion to FN (**Fig. 2A**). Robust spreading defects were not observed for any other Itg-KD cells on FN. A large proportion of Itg $\beta$ 1-KD cells failed to attach on Col I and LN-511 substrates and those which survived washing steps showed impaired spreading (**Fig. 2B–C**). Itg $\alpha$ V-KD cells had a marked spreading defect on both Col I and LN-511, providing a likely explanation for their detachment in the cell washing assay. None of the potential  $\alpha$ V-pairing  $\beta$ -subunit ( $\beta$ 3,  $\beta$ 5,  $\beta$ 6 or  $\beta$ 8) KDs showed significant cell spreading defects on Col I or LN-511 (**Fig. 2B–C**). Thus, depletion of multiple Itg $\alpha$ V-integrin containing heterodimers (Itg $\alpha$ V-KD cells) is required to impair cell spreading on these substrates.

To confirm that  $\alpha$ V-integrin function underlies the observed cell spreading defect we transduced the MDCK cell line that stably expresses human  $\alpha$ V-integrin-RFP with control and the two Itg $\alpha$ V-KD constructs to silence the expression of endogenous canine  $\alpha$ V-integrin. The knockdown efficiencies were confirmed both at protein and mRNA level (**Fig. 2D**, see also Fig. S1A). Itg $\alpha$ V-shRNA#1-construct contains multiple mismatches with the human  $\alpha$ V-integrin mRNA and it was ineffective in silencing the ectopically expressed human  $\alpha$ V-integrin mRNA that consequently rescued cell spreading in Itg $\alpha$ V-shRNA#1 transduced cells on all of the studied substrates (**Fig. 2E**). On the contrary, Itg $\alpha$ V-shRNA#2 contains only one mismatch with the human  $\alpha$ V-integrin sequence close to the 3'-end of the target sequence and it is expected to significantly reduce the expression of not only the endogenous canine  $\alpha$ V-integrin but also the ectopically expressed human  $\alpha$ V-integrin-RFP [35]. Indeed, Itg $\alpha$ V-shRNA#2 efficiently down-regulated the expression of human  $\alpha$ V-integrin-RFP protein thereby leading to cell spreading defect on Col I, LN-511 and FN (**Fig. 2D–E**). We also tested the effect of  $\alpha$ V-integrin depletion on the spreading of some other cell lines. Although the spreading of MK3 cells, a cell line derived from mouse embryonic kidney, was somewhat less pronounced on collagen substrate when compared with MDCK cells, a significant reduction in spreading of MK3 cells was seen upon depletion of  $\alpha$ V-integrin expression

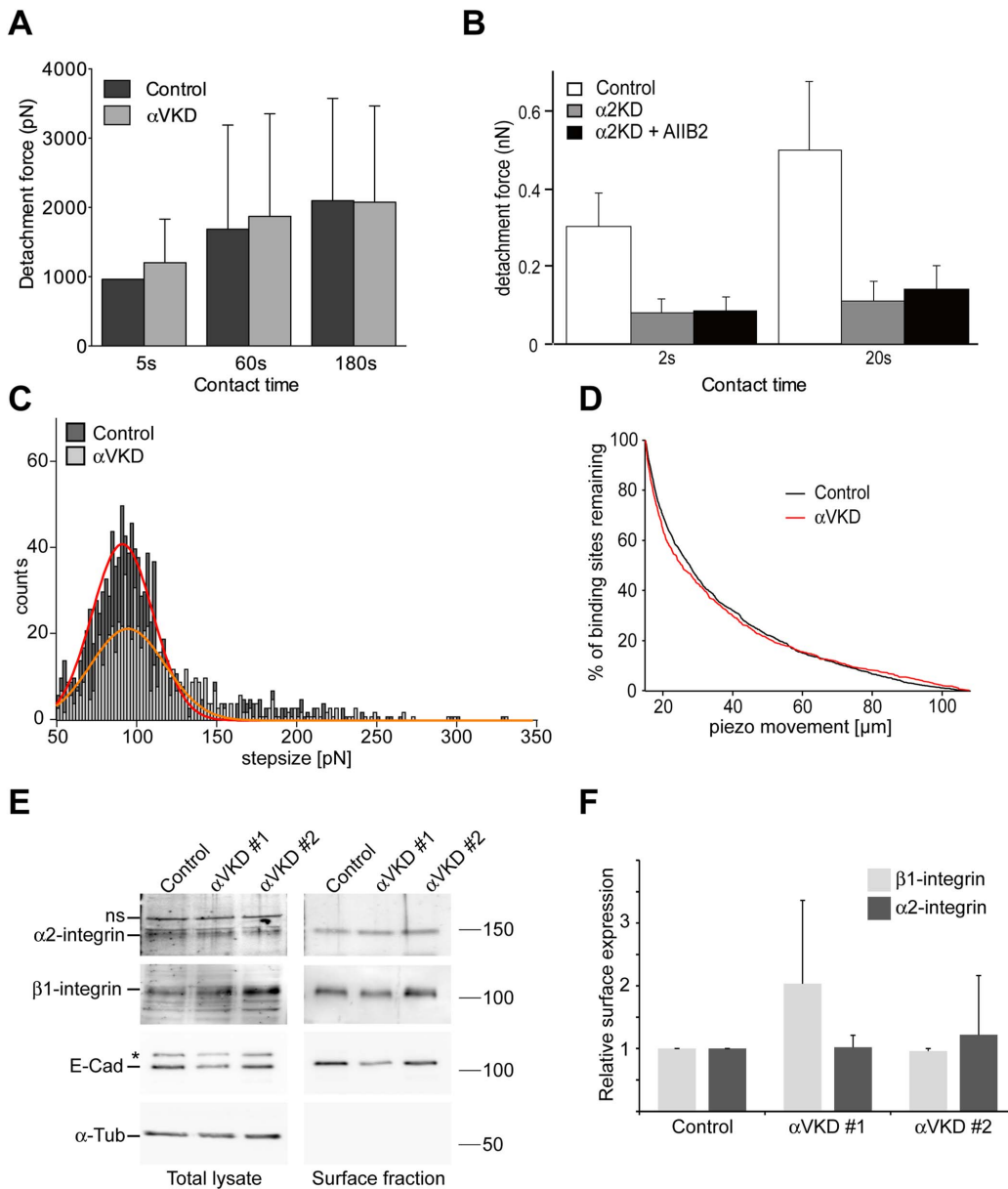


**Figure 1.  $\alpha$ V-integrins do not contribute to early adhesion to collagen I in MDCK cells.** **A)** Quantifying early cell adhesion by SCFS. Single control or Itg $\alpha$ V-KD cells were captured onto ConA-coated AFM cantilevers and pressed onto Col I-coated substrates. After the indicated contact times, cells were lifted from the substrate, and the maximum detachment force was recorded as described in materials and methods. More than 100 F–D curves were recorded for each condition. Mean+SD is shown. **B)** The maximum detachment force between collagen I substrate and control or Itg $\alpha$ 2-KD MDCK cells was measured in the absence and presence of antibodies that block  $\beta$ 1-integrin adhesion (A11B2). At least 20 cells were analyzed for each condition. Values show mean  $\pm$  SD. Membrane tether analysis (see T in Fig. S3A): **C)** The distributions of tether rupture forces for control and Itg $\alpha$ V-KD cells both center at a value of  $\approx$ 92 pN, indicating no differences in cell membrane properties. 78 F–D curves for control and 41 F–D curves for Itg $\alpha$ V-KD cells were analyzed. **D)** Membrane tether length analysis of control and Itg $\alpha$ V-KD cells to identify possible differences of receptor affinity and cell membrane-cortex interactions. A very similar tether length distribution does not indicate any changes. To assure that analyzed rupture events exclusively originated from membrane tethers force steps within 7  $\mu$ m after the maximum detachment force were omitted from analysis. **E)** Control and two independent Itg $\alpha$ V-KD MDCK cell lines were allowed to spread on Col I-coated plastic tissue culture dishes for 75 minutes followed by surface biotinylation. After cell lysis, biotin-bound molecules were precipitated with avidin-beads and relative amounts of  $\beta$ 1- and  $\alpha$ 2-integrins in biotinylated vs. total lysates were determined by SDS-PAGE and western blotting as described in materials and methods. E-Cadherin (E-Cad, asterisk indicates an intracellular precursor of E-Cad) and  $\beta$ -actin were used as biotinylation and loading controls. ns = non-specific. **F)** Quantification of the relative surface expression of  $\beta$ 1- and  $\alpha$ 2-integrins in the indicated cell lines. doi:10.1371/journal.pone.0071485.g001

(Fig. S4). In addition,  $\alpha$ V-integrin depleted human umbilical vein endothelial cells displayed a spreading defect on Col I substrate (data not shown).

$\alpha$ V-integrins regulate the dynamics of  $\beta$ 1-integrin-mediated focal adhesions

To study cell spreading dynamics in more detail we performed timelapse imaging of control, Itg $\alpha$ V- and Itg $\beta$ 1-KD MDCK cells

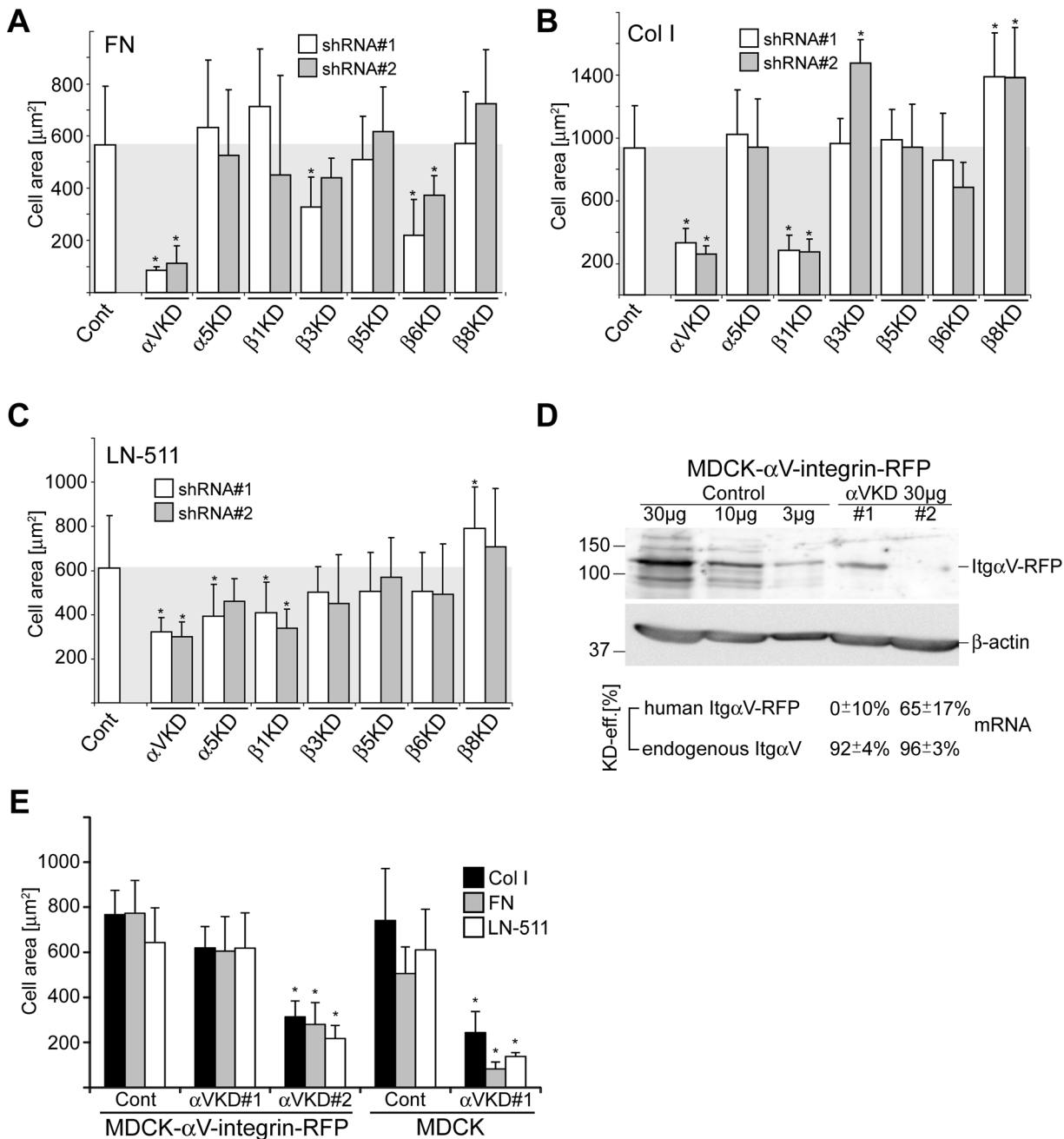


**Figure 2.  $\alpha$ V-integrins are required for efficient cell spreading on multiple ECM substrates.** Control and the indicated Itg-KD MDCK cells were plated on **A**) fibronectin-, **B**) Col I- or **C**) LN-511-coated glass coverslips and allowed to spread for 75 minutes. Cells were fixed and filamentous actin was stained using TRITC-Phalloidin. The combined data shows the mean cell spreading area ( $\mu\text{m}^2/\text{cell}$ ) +SD of 3–6 independent experiments. For each experiment and coating condition 60–150 cells from 10–30 frames were analyzed. **D**) MDCK cells stably expressing human  $\alpha$ V-integrin-RFP fusion protein were transduced with control, Itg $\alpha$ V-KD#1 or Itg $\alpha$ V-KD#2 shRNA-expressing viral vectors. The indicated amounts of total cell lysates were loaded onto SDS-PAGE followed by detection of human  $\alpha$ V-integrins by western blotting (upper panel). Actin was used as a loading control (lower panel). KD-efficiencies for both endogenous and ectopically expressed  $\alpha$ V-integrins were also determined using qPCR. Note that human  $\alpha$ V-integrin is resistant to silencing by shRNA#1 but not shRNA#2 whereas both shRNAs efficiently silence the expression of canine  $\alpha$ V-integrin (see also Fig. S1). **E**) The spreading of the different MDCK- $\alpha$ V-integrin-RFP cell lines on Col I, FN and LN-511 was analyzed as above together with control and Itg $\alpha$ V-KD#1 MDCK cells. The data shows the mean cell spreading area +SD from 2 independent experiments performed in triplicates. P-values <0.01 are signified by (\*). doi:10.1371/journal.pone.0071485.g002

stably expressing GFP-talin or GFP-vinculin on Col I substrates. Talin binding to the cytoplasmic domain of  $\beta$ 1-integrins is considered as an early event depicting integrin activation leading to the formation of focal complexes (FXs) whereas accumulation of

vinculin is thought to occur upon stabilization of focal adhesions (FAs) due to robust linkage to actin cytoskeleton [34,36]. The half-life of GFP-positive pericellular foci was analyzed in the different Itg-KD cell lines. Upon initial contact, control cells protruded

prominent lamellipodia which progressively stabilized leading to cell spreading and flattening of the cell body (**Movie S1**). Both GFP-talin and GFP-vinculin were efficiently recruited to peripheral foci most of which persisted for ~60 minutes (**Fig. 3A**). In contrast, the lamellipodia in Itg $\alpha$ V-KD cells went through continuous protrusion-retraction cycles and showed reduced amount of GFP-talin positive foci that were more short-lived (<40 minutes; **Movie S2**) than in controls. The average residence time of GFP-vinculin in these foci was even shorter (10–20 minutes; **Movie S3**). Similar to Itg $\alpha$ V-KD cells, only short-lived dynamic GFP-vinculin- or GFP-talin-positive foci were visible in Itg $\beta$ 1-KD cells (**Fig. 3A**). Curiously, unlike Itg $\alpha$ V-KD cells where the spreading phenotype persisted, overnight cultures of Itg $\beta$ 1-KD cells eventually formed stable vinculin-positive adhesive structures and spread (data not shown). This is possibly due to secretion and assembly of endogenous ECM, such as LN-511 or FN that can be bound by other integrins and non-integrin receptors [37]. These data show that  $\alpha$ V-integrins are required to stabilize  $\alpha$ 2 $\beta$ 1-integrin-mediated FAs on Col I.

**$\alpha$ V-integrins are required for efficient maturation of FAs**

The maturation of FXs to FAs and ultimately to fibrillar adhesions is a complex and highly orchestrated process [38]. We studied the recruitment of selected FA components to the maturing FXs by analyzing the number and average size of peripheral foci immunostained with these selected markers (**Fig. 3B, C**). Efficient clustering of  $\beta$ 1-integrins at lamellipodia was observed in control cells (**Fig. 4A**).  $\beta$ 1-integrin clusters were observed also in Itg $\alpha$ V-KD cells although they were significantly less in number than those in control cells (**Fig. 4A**). In agreement with the GFP-talin data, endogenous talin was recruited to clearly distinguishable foci at FAs in control cells whereas it was rarely seen to accumulate in adhesions in Itg $\alpha$ V-KD cells or Itg $\beta$ 1-KD cells (**Fig. 4B**). Paxillin, another proximal  $\beta$ 1-integrin-binding protein, was recruited to small peripheral foci that aligned with the ends of actin stress fibers in control cells but only few diffuse structures were seen in Itg $\alpha$ V- and Itg $\beta$ 1-KD cells (**Fig. 4C**). In agreement with timelapse experiments, the number of vinculin-positive FAs was significantly reduced in both Itg $\beta$ 1- and Itg $\alpha$ V-KD cells when compared with control cells (**Fig. 4D**). Thus it appears that Itg $\alpha$ V-KD cells adhere to Col I via  $\alpha$ 2 $\beta$ 1-integrins but these early  $\beta$ 1-integrin-positive foci do not properly mature into FAs.

Mechanical forces acting upon cytoskeleton and cell-matrix contacts play an important role in FA maturation [34]. Forces generated by actomyosin contractility recruit zyxin to FAs where it regulates actin polymerization [39,40]. In control cells, zyxin was robustly recruited to maturing FAs and aligned with adjacent stress fibers (**Fig. 4E**). Unlike the elongated sharp-edged structures in control cells, zyxin stained diffuse clusters in some Itg $\beta$ 1-KD cells or was cytoplasmic in others (**Fig. 4E**). In Itg $\alpha$ V-KD cells zyxin did not show any evident clustering (**Fig. 4E**). Integrin-linked kinase (ILK), together with its binding partners PINCH1 and  $\alpha$ -parvin, is thought to strengthen the interactions between integrins and F-actin thereby preventing disruption of the ECM-cytoskeleton linkage under mechanical stress [41,42]. We generated MDCK cells stably expressing an GFP-ILK fusion protein [43]. GFP-ILK accumulated at FA and aligned with actin stress fibers in control cells (**Fig. 4F**). In contrast, in Itg $\beta$ 1- and Itg $\alpha$ V-KD cells GFP-ILK recruitment to FAs was severely affected (**Fig. 4F**). Defective FA-recruitment of these factors in Itg $\alpha$ V-KD cells suggests that the linkage between the ECM-bound  $\beta$ 1-integrins and the actin cytoskeleton is impaired.

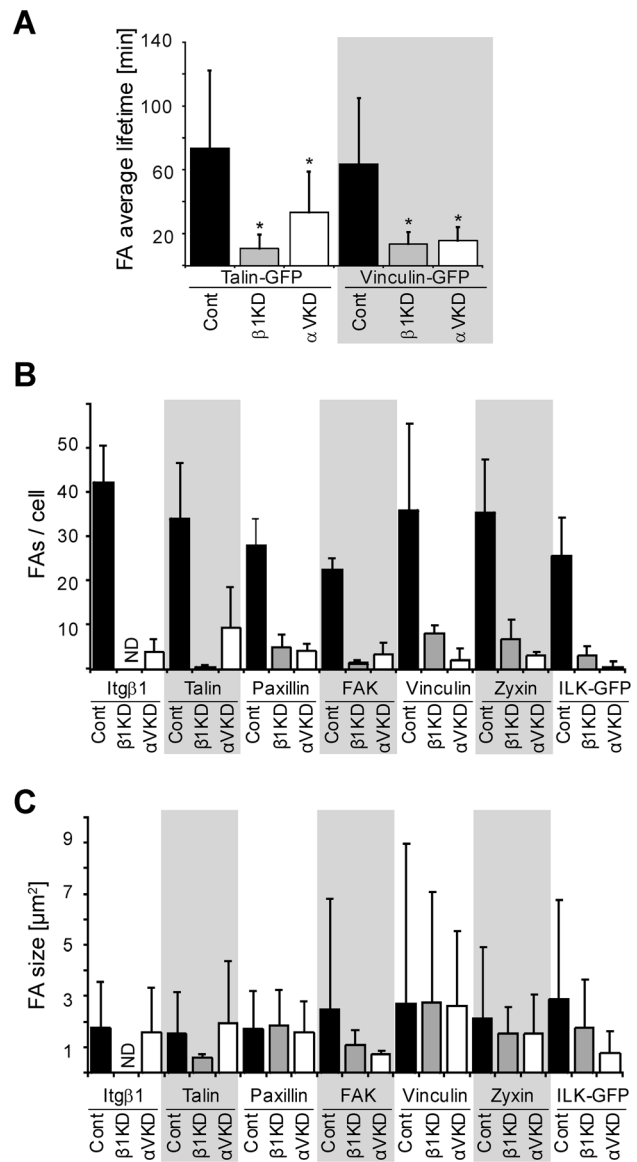


**Figure 3.  $\beta$ 1-integrin-mediated focal complexes form but do not mature on collagen I in the absence of  $\alpha$ V-integrins.** **A**) Control, Itg $\beta$ 1- and Itg $\alpha$ V-KD MDCK cells stably expressing GFP-talin (**Movie S2**) or GFP-vinculin (**Movie S3**) were trypsinized and seeded onto Col I-coated glass-bottom petri dishes in serum-free culture medium. Cells were allowed to react with the substrate for 30–60 minutes after which the dynamics of FAs were imaged using timelapse microscopy. Images were acquired every 3 minutes and the average lifetime of FAs was determined as described in materials and methods. More than 50 FAs were tracked per each condition. P-values <0.01 are signified by (\*). **B**) Control, Itg $\beta$ 1- and Itg $\alpha$ V-KD MDCK cells were trypsinized, seeded onto Col I-coated coverslips, allowed to settle for 75 minutes, fixed and stained for the indicated FA markers. The number and **C**) the average size of FAs with each of these markers were analyzed as described in materials and methods. For each sample 5–15 cells were analyzed and the data show mean+SD combined from 3 independent experiments. ND: not detectable.  
doi:10.1371/journal.pone.0071485.g003

Talin and paxillin are thought to contribute to the recruitment of focal adhesion kinase (FAK) to regulate the maturation of FAs [44] whereas ILK interacts with the cytoplasmic tails of  $\beta$ 1- and  $\beta$ 3-integrins to link FAs to actin cytoskeleton and thereby promote FA maturation [45,46]. FAK was efficiently recruited to FAs in

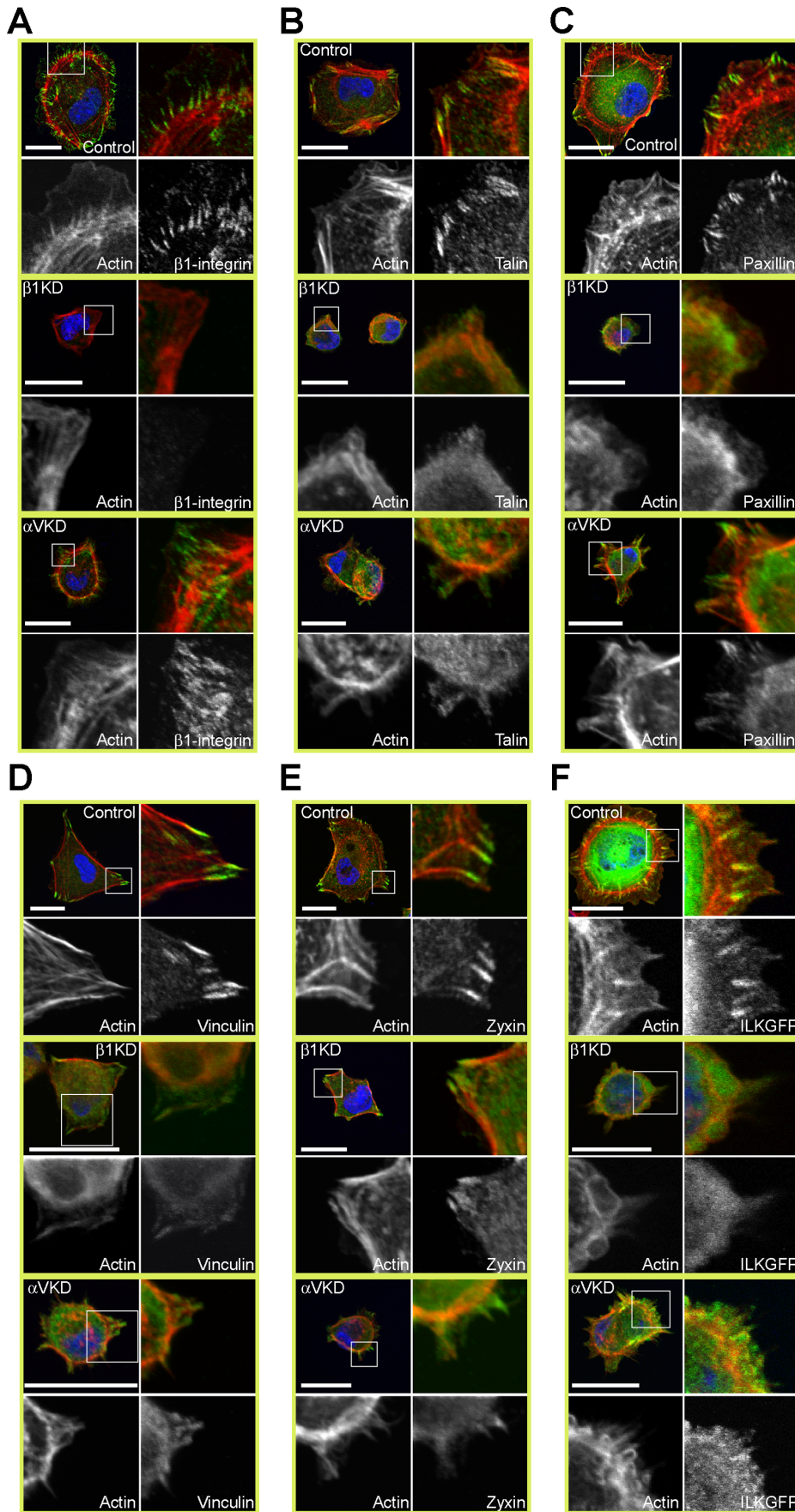


**Figure 4. Recruitment of multiple FA components is defective in Itg $\alpha$ V- and Itg $\beta$ 1-KD ItgV-KD cells.** **A)** Control, Itg $\beta$ 1- and Itg $\alpha$ V-KD MDCK cells were trypsinized, seeded onto Col I-coated coverslips in serum-free culture medium, allowed to settle for 75 minutes, fixed and stained for actin (TRITC-phalloidin, red), nuclei (DAPI, blue) and  $\beta$ 1-integrin (green). **B)** talin, **C)** paxillin, **D)** vinculin or **E)** zyxin. **F)** Control, Itg $\beta$ 1- and Itg $\alpha$ V-KD MDCK cells expressing GFP-ILK (green) were treated as above and stained for actin (TRITC-phalloidin, red) and nuclei (DAPI, blue). Scale bars are 20  $\mu$ m in all figure panels.  
doi:10.1371/journal.pone.0071485.g004

control MDCK cells whereas limited a number of poorly organized FAK-positive foci were observed in Itg $\beta$ 1-KD cells and only diffuse lamellipodial FAK-staining in Itg $\alpha$ V-KD cells (**Fig. 3B, C and 5A**). Integrin clustering induces phosphorylation of FAK on the pTyr<sup>397</sup>-residue which provides a docking site for cellular proto-oncogene tyrosine-protein kinase (c-Src) and facilitates its activation (pTyr<sup>418</sup>) [47]. The resulting FAK/c-Src dual kinase complex activates multiple signals downstream of integrin activation [48]. Surprisingly, despite the different appearance of the FAK-localization in the Itg $\beta$ 1-KD cells the depletion of  $\beta$ 1-integrin did not reduce specific FAK or c-Src activation and instead a tendency for slightly elevated activity was noted in cells analyzed 75 minutes after seeding when compared with control cells (**Fig. 5B, C**). Despite normal c-Src-activation, Itg $\alpha$ V-KD cells failed to efficiently activate FAK upon adhesion to Col I (**Fig. 5B, C**).

To study the relative contribution of selected key components in FA maturation we generated talin-1 (Tln1)-, FAK- and ILK-KD MDCK cells and analyzed their spreading on Col I and LN-511 substrates. The KD-efficiencies were determined by qPCR (Tln-1, FAK and ILK; **Table S1A**). All of these KDs inhibited cell spreading on Col I substrate (**Fig. 5D**) and all but one of the two ILK-KD constructs impaired cell spreading on LN-511 (**Fig. 5E**). These data show that the failure of Itg $\alpha$ V-KD cells to recruit talin, FAK, and ILK to the forming adhesion on Col I substrate could underlie the cell spreading phenotype.

### Cellular mechanotransduction processes are defective in Itg $\alpha$ V-KD MDCK cells

Integrin-mediated FAs function as cellular sensors to monitor the rigidity of the extracellular environment [34]. Because  $\alpha$ V-integrins were found to be involved in the maturation of FAs their potential role in mechanotransduction was studied. To modulate substrate rigidity in vitro we used stiff ( $1893 \pm 394$  Pa; 10% PAA) and soft ( $212 \pm 9$  Pa; 3% PAA) polyacrylamide (PAA) gels that were coated with the same concentration of Col I [49]. The different cell lines were incubated on the substrates overnight. Control cells spread efficiently when allowed to settle on stiff Col I-coated gels whereas on soft substrates they did not flatten (**Fig. 6A**). On the other hand, Itg $\alpha$ V-KD cells had roundish “soft” morphology irrespective of the substrate rigidity (**Fig. 6A**). Janmey et al. reported that cells re-organize the actin cytoskeleton to increase their elastic properties in response to increasing substrate stiffness [50]. Thus, if the mechanotransduction machinery in Itg $\alpha$ V-KD cells is defective these cells would be softer than control cells on a rigid surface. Control and Itg $\alpha$ V-KD cells were seeded onto a stiff Col I-coated glass coverslip and allowed to adhere for 12 hours. Upon prolonged exposure on stiff surface, some Itg $\alpha$ V-KD cells flattened transiently. Quantitative cell elasticity measurements on such flattened Itg $\alpha$ V-KD cells in comparison with control cells were performed using AFM (**Fig. 6B**). Control cells had a rather broad spectrum of elasticities ranging from 100 to 1000 Pa (Young’s modulus) with a mean value of 267 Pa when probed with 5  $\mu$ m beads and 186 Pa when using larger 20  $\mu$ m beads. Itg $\alpha$ V-KD cells were significantly softer with mean values of 130 Pa regardless of the bead size used, indicating that they did not respond to the substrate stiffness.

To directly measure the maturation of FAs upon mechanical stimulus we probed control and Itg $\alpha$ V-KD cells with a Col I-coated bead attached to an AFM cantilever (**Fig. S3B**). Cells were allowed to bind the bead for 2 minutes. Then, the bead was oscillated at a frequency of 0.25 Hz and an amplitude of 200 nm for 20 minutes. During oscillation, the bead was retracted to stress the attached cell and the force acting on the cantilever was measured. Repeated pulling of the bead consistently increased the mechanical response of the stressed control cells whereas the mechanical force response of Itg $\alpha$ V-KD cells decreased (**Fig. 6C**). The increasing mechanical resistance to bead movement in control cells likely represents the strengthening of the linkage between the FAs forming on the bead and the cellular actin cytoskeleton [15].

To dissect further which of the FA components contribute to mechanosensory responses we seeded talin-1-, FAK- and ILK-KD cells onto soft and stiff collagen-coated substrates and allowed them to grow on the substrates overnight. The depletion of talin-1 and FAK proteins were confirmed by western blotting (**Fig. 6D, E**). Whereas both talin-1-KD constructs shared the mechanotransduction defect seen with Itg $\alpha$ V-KD cells, FAK- and ILK-KD cells retained their capacity to spread on stiff Col I-coated substrate after overnight incubation implicating talin-1 as a critical component of the mechanosensory machinery in MDCK cells (**Fig. 6F**).

### Discussion

Functional characterization of RGD-motif binding integrins in MDCK cells revealed that  $\alpha$ V $\beta$ 6-integrin is the main adhesion receptor for RGD-containing FN while both  $\alpha$ V $\beta$ 6 and  $\alpha$ V $\beta$ 3-integrins contributed to cell spreading on FN substrate. Importantly, we observed that depletion of  $\alpha$ V-integrins led to a marked cell spreading defect also on Col I and LN-511. Although  $\alpha$ V-integrins reportedly can bind modified or denatured collagen [51] we did not observe significant  $\alpha$ V-integrin-mediated binding to Col I in our experimental setups. Moreover,  $\alpha$ V-integrins were not essential for the cell surface expression of  $\alpha$ 2 $\beta$ 1-integrins which mediated Col I binding both in the presence and absence of  $\alpha$ V-integrins. However, recruitment of talin, vinculin, ILK and zyxin to the forming adhesions as well as activation of FAK were abrogated in Itg $\alpha$ V-KD cells. Consequently,  $\beta$ 1-integrin-mediated adhesions on Col I substrate did not properly link to cellular cytoskeleton leading to defective FA maturation and impaired mechanosensory responses. We showed that expression of talin-1, but not FAK or ILK, was required for efficient mechanosensory responses in MDCK cells.

Our data reveals a presumably indirect functional cooperation between  $\alpha$ 2 $\beta$ 1- and  $\alpha$ V-integrins during MDCK cell spreading. Here, several scenarios are possible. One of the best understood examples of integrin cross-regulation is between  $\alpha$ V $\beta$ 3- and  $\alpha$ 5 $\beta$ 1-integrins, both of which bind to FN. Ligation and rapid recycling of  $\alpha$ V $\beta$ 3 slows down surface transport of  $\alpha$ 5 $\beta$ 1 from the perinuclear recycling compartment thereby promoting persistent migration of fibroblasts [17]. Inhibition of  $\alpha$ V $\beta$ 3-function results in increased surface exposure of  $\alpha$ 5 $\beta$ 1-integrin which in turn facilitates random migration and invasiveness of fibroblasts and ovarian carcinoma cells [52]. We did not observe significant

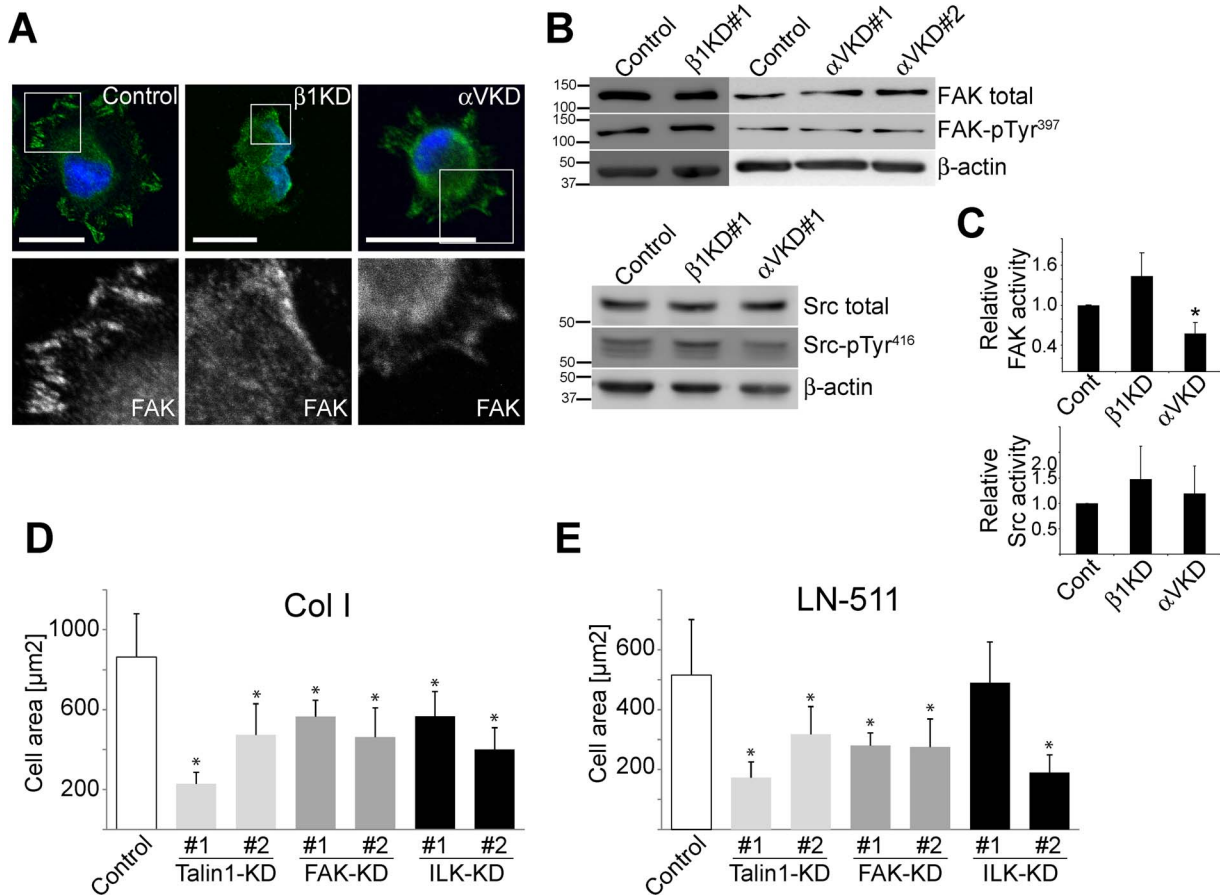


**Figure 5.  $\alpha$ V-integrins are required for proper FAK activation that together with talin-1 and ILK regulates MDCK cell spreading on Col I.** **A**) Control, Itg $\beta$ 1- and Itg $\alpha$ V-KD MDCK cells were trypsinized, seeded onto Col I-coated coverslips in serum-free culture medium, allowed to settle for 75 minutes, fixed and stained for actin (TRITC-phalloidin, red), nuclei (DAPI, blue) and FAK (green). Scale bars are 20  $\mu$ m. **B**) Control, Itg $\beta$ 1- and Itg $\alpha$ V-KD MDCK cells were trypsinized and seeded onto Col I-coated culture dishes. After 75 minutes cells were lysed and post-nuclear lysates were loaded onto SDS-PAGE followed by detection of total FAK and phosphorylated (pTyr<sup>397</sup>) FAK protein levels as well as total c-Src and phosphorylated (pTyr<sup>416</sup>) c-Src protein levels in the three cell lines. **C**) Quantitation of the FAK and c-Src activation in control, Itg $\beta$ 1- and Itg $\alpha$ V-KD cells. The intensity ratios of FAK-pTyr<sup>397</sup>/FAK and c-Src-pTyr<sup>416</sup>/c-Src were quantified as described in material and methods from 3 independent experiments. Data is shown as mean+SD. **D**) Control, talin-1, FAK- and ILK-KD MDCK cells were plated on Col I- or **E**) LN-511-coated glass coverslips and allowed to spread for 75 minutes. Cells were fixed and filamentous actin was stained using TRITC-Phalloidin. The combined data shows the mean cell spreading area ( $\mu$ m<sup>2</sup>/cell)+SD of 3 independent experiments. For each experiment and coating condition 60–150 cells from 10–30 frames were analyzed. P-values <0.01 are signified by (\*). doi:10.1371/journal.pone.0071485.g005

changes in the surface exposure of  $\alpha$ 2 $\beta$ 1-integrin in Itg $\alpha$ V-KD cells. However, because the trafficking of  $\beta$ 1-integrins was not addressed in detail in our study we cannot exclude that some  $\beta$ 1-integrin recycling defects occur in Itg $\alpha$ V-KD cells.

An elegant recent study identified separate roles for  $\alpha$ 5 $\beta$ 1- and  $\alpha$ V $\beta$ 3-integrins in fibroblasts adhering to FN. It was reported that  $\alpha$ 5 $\beta$ 1-integrins determine adhesion strength whereas  $\alpha$ V $\beta$ 3-integrins enable mechanotransduction [15]. Both  $\alpha$ 5 $\beta$ 1- and  $\alpha$ V $\beta$ 3-integrins were required for proper maturation of FXs into FAs. After initial co-localization at FX,  $\alpha$ 5 $\beta$ 1-integrin gradually accumulated and formed more stable mature FAs behind lamellipodia while  $\alpha$ V $\beta$ 3 remained at the leading lamella continuously probing the ECM. Our data implicating  $\alpha$ V-integrins as regulators of mechanical FA maturation while  $\beta$ 1-integrins mediate substrate binding appears compatible with these findings. Some earlier studies using modified fibroblast cell lines have reported that both  $\alpha$ V $\beta$ 3- and  $\alpha$ 2 $\beta$ 1-integrins can contribute to mechanical deformation of collagen gels independently of each other [53,54]. However, in these studies  $\alpha$ V $\beta$ 3-integrins were

reported to bind to Col I substrate whereas no significant  $\alpha$ V-integrin-mediated binding to Col I was observed in our experiments. Roca-Cusachs et al. reported that talin did not contribute to the adhesion strength but was required for mechanotransduction [15]. Curiously, although both Itg $\alpha$ V- and Itg $\beta$ 1-KD cells failed to recruit talin at FAs only Itg $\alpha$ V-KD cells displayed a mechanotransduction defect. A recent study reported that whereas talin-depleted mammary epithelial cells failed to recruit multiple FA components, such as vinculin and FAK, cell spreading was not compromised as the necessary linkage between FAs and the actin cytoskeleton might have been mediated by other molecules, such as tensin [55]. We observed that talin-1-KD MDCK cells failed to spread efficiently on stiff collagen substrate thereby suggesting that talin-1 is a critical component of the mechanosensory machinery in MDCK cells. It should be noted, however, that talin-1 is required for efficient integrin activation [56,57]. Further studies are needed to determine whether the spreading defect in talin-1-KD MDCK cells results from a general inhibition of integrin activation or if talin-1 might also have a more

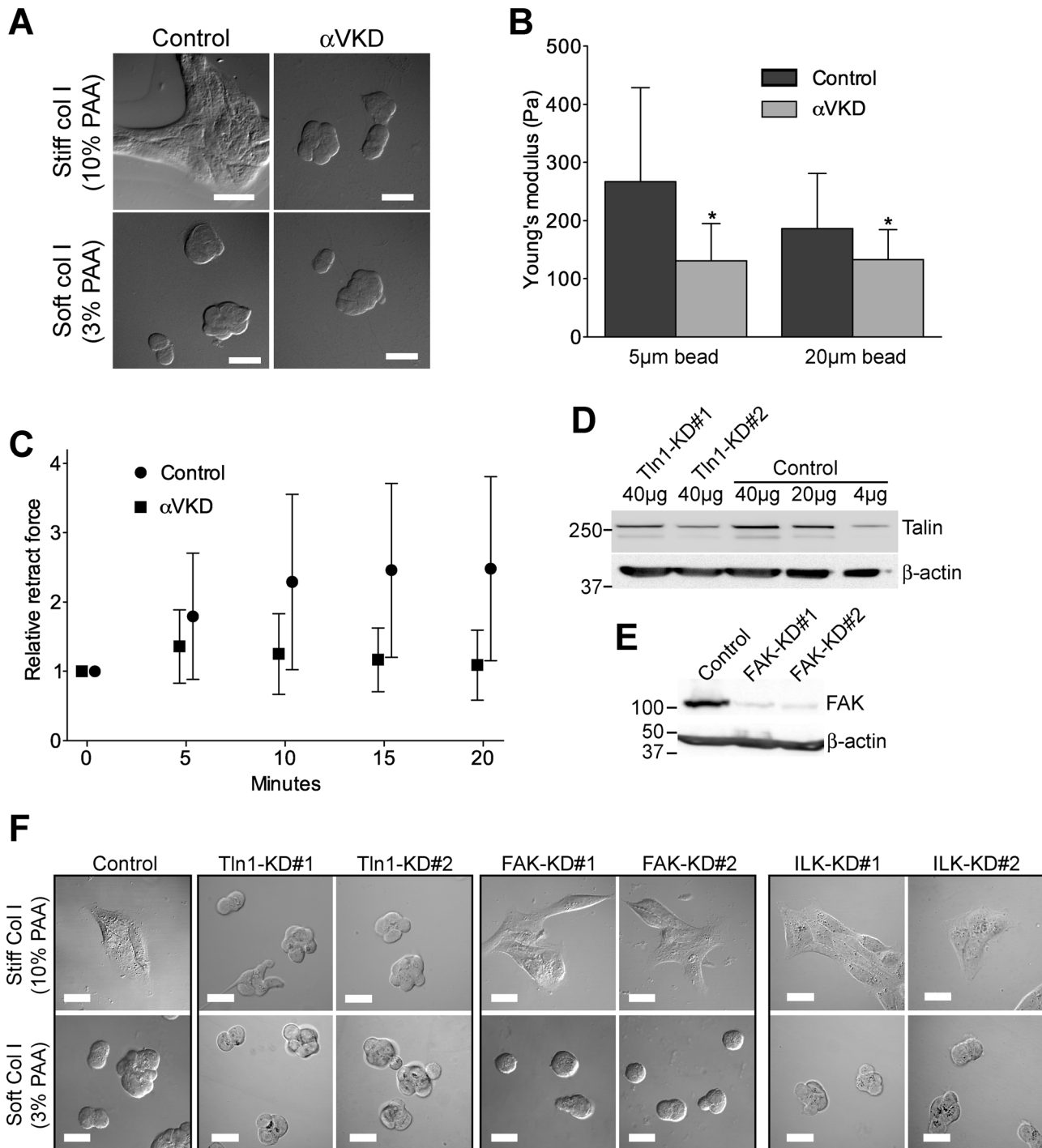


**Figure 6. Mechanotransduction processes are abrogated in Itg $\alpha$ V-KD MDCK cells.** A) Control and Itg $\alpha$ V-KD MDCK cells were trypsinized and seeded onto stiff (10% PAA) or soft (3% PAA) Col I-coated substrates. Cells were allowed to spread overnight followed by PFA-fixation and imaged using DIC-microscopy. Scale bars are 20  $\mu$ m. B) Determining the cell elasticity of control and Itg $\alpha$ V-KD cells. Cells were seeded onto Col I-coated substrate and allowed to bind and spread for 12 hours. Cell elasticity was probed with 5 or 20  $\mu$ m glass beads attached to an AFM cantilever. More than 60 cells per cell type and bead size were probed. Mean+SD is shown. P-values <0.01 are signified by (\*). C) Control and Itg $\alpha$ V-KD MDCK cells growing on Col I-coated substrate were probed with a 5  $\mu$ m bead attached to a tipless cantilever (Figure S3B). After making initial contact between Col I-coated bead and cell with a contact force of 1 nN for 120 seconds, the cantilever was oscillated at a frequency of 0.25 Hz and amplitude of 200 nm for 20 minutes. During oscillation, the force acting on the cantilever was recorded. More than 20 control and Itg $\alpha$ V-KD cells were analyzed. D) The indicated amounts of control and two independent talin (Tln)-1-KD cell line lysates were loaded for SDS-PAGE followed by western blotting with mouse anti-talin antibodies. E) Thirty micrograms of total lysates from control and two independent FAK-KD cell lines were loaded for SDS-PAGE followed by western blotting with mouse anti-FAK antibodies. F) Control and the indicated KD cell lines were trypsinized and seeded onto stiff (10% PAA) or soft (3% PAA) Col I-coated substrates. Cells were allowed to spread overnight followed by PFA-fixation and imaged using DIC-microscopy. Scale bars are 20  $\mu$ m.  
doi:10.1371/journal.pone.0071485.g006

specific role in cellular mechanotransduction. The differential dependence on talin-1 expression in the spreading of the two epithelial cell lines could be due to cell line specific effects but further studies are needed to clarify this discrepancy. Interestingly, in fibroblasts talin is not required for initial adhesion or formation of lamellipodial protrusions but is necessary for FA maturation and cell spreading [58].

Although  $\alpha$ V-integrins were found to regulate recruitment of several FA components and modulate activation of FAK, our data implicated talin, but not FAK or ILK, as a crucial FA component that regulates mechanosensory responses in MDCK cells. Further studies are warranted to characterize the detailed molecular mechanisms how  $\alpha$ V-integrins and talin-1 regulate maturation of  $\beta$ 1-integrin mediated FAs in MDCK cells.

## Materials and Methods

### Antibodies and ECM proteins

Rat anti- $\beta$ 1-integrin (AIB2, [59]), mouse anti- $\beta$ 1-integrin (TS2/16; [60]) and rabbit anti- $\beta$ 1-integrin [61] antibodies were kindly provided by Dr. K. Matlin (Department of Surgery, University of Chicago, Chicago, IL). Mouse anti- $\alpha$ 2-integrin (5E8; [62]) was kindly provided by Dr. R.B. Bankert (Department of Microbiology and Immunology, University at Buffalo, Buffalo, NY). Rabbit-anti  $\beta$ 1-integrin antibody was from Chemicon (ABI952). Mouse anti- $\alpha$ V $\beta$ 3-integrin (LS-C15967), rabbit anti- $\beta$ 6-integrin (LS-C24779) and sheep anti- $\beta$ 5-integrin (LS-C36943) antibodies were from Lifespan Biosciences. Mouse anti-talin (#T3287, clone 8D4), rabbit anti- $\alpha$ V-integrin (#6617) and mouse anti-vinculin (#4505) were from Sigma. Rabbit anti- $\alpha$ 2-integrin was from Santa Cruz (sc-9089). Mouse anti-paxillin (#AHO0492) was from Zymed. Mouse anti-FAK (#610088) was purchased from BD Transduction Laboratories<sup>TM</sup> and mouse anti-FAK (pTyr-397; #FM1211) from ECM Biosciences. Rabbit anti-Zyxin (ab1842) was purchased from Abcam. Cy2-, Cy3- and HRP-conjugated secondary antibodies were from Jackson Immuno-research and Alexa488-conjugated secondary antibodies were from Invitrogen. TRITC-Phalloidin and DAPI were purchased from Sigma. c-Src-antibody Sampler Kit (#9935) was purchased from Cell Signaling Technology. Bovine dermal collagen I (Pure-Col<sup>TM</sup>, Inamed), BME (Matrigel<sup>TM</sup>, BD biosciences) and placental laminin-511 (Sigma, L6274; [63]) were purchased.

### Cell culture and treatments

For 2D culture, MDCK cells were grown in minimum essential medium (MEM, Invitrogen) supplied with 5% fetal bovine serum (FBS) and 1% penicillin/streptomycin at +37°C in a humidified CO<sub>2</sub>-incubator. Mouse kidney mesenchyme (MK3) cells were grown in Dulbecco's modified Eagle's medium (DMEM, 4,5 g glucose/l, Invitrogen) supplemented with 5% FBS [64].

### Generation of knockdown and overexpression cell lines

Knockdown cells were created as described previously [65]. Two functional constructs (>70% KD efficiency as determined by qPCR) were generated for each gene. For the target sequences and oligos used for qPCR see Table S1. When indicated, individual integrin-KD shRNA-expressing MDCK cell clones were picked and expanded. GFP-Talin1 ([66], Addgene plasmid 26724), GFP-vinculin [67], GFP-ILK [43] and  $\alpha$ V-integrin-TagRFP (Evrogen JSC, #FP361) expressing cell lines were generated by stable transfection using Amaxa nucleofection (Lonza GmbH), individual colonies were picked. When indicated, the resulting cell clones were subsequently transduced with the integrin-targeting shRNA constructs.

### Cell washing assay

Subconfluent cells were washed two times with PBS and once with PBS containing 2 mM EDTA/0.5 mM EGTA after which the cells were detached using MEM containing 4 mM EDTA/1 mM EGTA. Detached cells were centrifuged (1000rpm, 3 min, at RT) and resuspended at a density of  $2 \times 10^6$  cells/ml into MEM (w/o serum).  $10^5$  cells per well were pipetted onto a 96-well plates and let to adhere for 90 minutes. Wells were coated with Col I (30  $\mu$ g/ml), fibronectin (10  $\mu$ g/ml), LN-511 (10  $\mu$ g/ml) or BME (90  $\mu$ g/ml) and blocked with 1% BSA as described [24]. Non-adherent cells were removed by washing four times with PBS containing 0.9 mM calcium and 0.49 mM magnesium (PBS<sup>+</sup>). Remaining adherent cells were fixed with methanol and stained with 0.1% crystal violet. Cells were lysed in 0.1% sodium deoxycholate/10 mM HEPES pH7 and absorption was measured at 544 nm.

### Cell spreading and FA assays

Cells were trypsinized and resuspended into serum-free MEM.  $1.5-2 \times 10^3$  cells were seeded onto 120mm coverslips and allowed to settle for 65–75 minutes. Coverslips were coated with Col I (3–30  $\mu$ g/ml), fibronectin (10  $\mu$ g/ml), LN-511 (5–10  $\mu$ g/ml) or basement membrane extract (90  $\mu$ g/ml) and blocked with 1% BSA prior to experiments. Specimens were washed with PBS<sup>+</sup>, fixed with 4% PFA in PBS<sup>+</sup> and stained with DAPI and TRITC-phalloidin. Cells were imaged with an Olympus FV-1000 confocal microscope. The average cell areas in ten individual field-of-views (40xobjective) were determined using ImageJ [68].

For FA analysis the number and size distribution of FAs were determined using the ImageJ software. In short, background was subtracted using the rolling ball algorithm and the images were thresholded to highlight FA clusters. Cell centers were omitted from the analysis due to high background fluorescence and the outer regions of the cells were examined using particle analysis application to segment and measure the number and the average size of FAs. Only objects larger than 0.5  $\mu$ m<sup>2</sup> in size were included into the analysis. Five to fifteen cells per condition were analyzed. For analysis of FA dynamics the MJTrack plugin of the ImageJ was used to track randomly selected FAs in the timelapse series where images were captured every 3 minutes [69]. Between fifty-three to seventy-nine FAs were analyzed per each condition and the average FA lifetimes in minutes were determined.

### Single-cell force spectroscopy

SCFS was performed on an AFM (NanoWizard, JPK Instruments) equipped with a CellHesion module (JPK Instruments) mounted on an inverted optical microscope (Axiovert 200 M, Zeiss, Jena, Germany). Measurements were performed in media (MEM supplemented with 25 mM Hepes) at 37°C, controlled by a PetriDishHeater (JPK Instruments). Tipless, 200  $\mu$ m long V-shaped cantilevers having nominal spring constant of 0.06 N/m (NP-O, Bruker) were calibrated using the equipartition theorem [70]. For SCFS, Ø35 mm glass-bottom petri dishes (WPI) were coated with Col I (PureCol<sup>TM</sup>, Nutacon) as described [29]. AFM cantilevers were plasma-cleaned and coated with concanavalin A (ConA, Sigma, 2 mg/ml) overnight at 4°C. When indicated, rat anti- $\beta$ 1-integrin antibody (AIB2–1:10 dilution of hybridoma supernatant) was incubated with cells 20 minutes prior to SCFS experiments. To attach a single cell to the cantilever, cell suspensions were pipetted onto the collagen-coated supports. The apex of a ConA-functionalized cantilever was lowered at a velocity of 10  $\mu$ m/s onto a cell until detecting a force of 1 nN. After a contact time of 5 s, the cantilever was withdrawn 90  $\mu$ m and the cantilever-bound cell was left for incubation for >10 min.

Then, the cantilever-bound cell was brought into contact with the collagen-coated support at a contact force of  $\approx 2$  nN for 5, 60 or 180 s. The approach and retract velocity of the cell was 5  $\mu\text{m/s}$ . The deflection of the cantilever was recorded and plotted as force-distance (F–D) curves. After recording 25–35 F–D curves, the cell on the cantilever was replaced and after 40–60 F–D curves the support was exchanged. Each dataset was generated using 20–25 cells. The maximum detachment force required to separate cell and support was extracted from retraction F–D curve using the AFM data processing software (JPK Instruments). Tether rupture forces and tether lengths were extracted from retraction F–D curves using in-house algorithms in Igor Pro 6.12 (WaveMetrics, Oregon, USA). Unbinding events within 7  $\mu\text{m}$  after the maximum detachment force were excluded from tether analysis.

### AFM-based nanoindentation experiments

The Young's moduli of cells and PAA gels were determined by AFM-based nanoindentation measurements. Before measurements, cells were seeded onto collagen-coated  $\text{O}35$  mm glass-bottom petri dishes (WPI) and incubated for 12 hours. PAA gels were formed as surface bound layers with a final thickness (swollen state) of approx. 200  $\mu\text{m}$ . After polymerization, each gel sample was washed in PBS to remove any non-bound polymeric precursors. Measurements were conducted at 37°C in PBS using a PetriDishHeater<sup>TM</sup> (JPK Instruments) sample chamber.

Colloidal force probes were prepared by attaching glass beads (Kisker Biotech) of various diameters (5 and 20  $\mu\text{m}$  for cell measurements; 10  $\mu\text{m}$  for PAA gel measurements) to the apex of tipless silicon nitride cantilever (NP-O, Bruker) using a two-component epoxy glue (Araldite) as described [70]. Spring constants of the colloidal probes were calibrated before measurements using the equipartition theorem [71]. To prevent non-specific adhesion, the modified cantilevers were incubated in heat inactivated FBS (Invitrogen) for 1 hour prior to measurements. For nanoindentation measurements, the approach and retract velocity was set to 1  $\mu\text{m/s}$ , the contact force to 0.5 nN, and the pulling range was 2  $\mu\text{m}$ . Experiments were performed in closed-loop, constant height mode. For cell measurements, up to three F–D curves, with at least 15 s waiting time between successive curves were recorded per cell. For PAA gel measurements, at least 100 different spots on 3 different samples were analysed. The data processing software provided by the AFM manufacturer (JPK Instruments) was used to extract the Young's Modulus  $E$  from approach force-distance curves. The software applies a modified Hertzian fit assuming a spherical indenter.

### Measuring mechanical maturation of FA using AFM

Cells were seeded onto collagen-coated  $\text{O}35$  mm glass-bottom petri dishes (WPI) and incubated for 12 hours. Colloidal force probes were prepared by attaching a 5  $\mu\text{m}$  glass bead to the apex of a tipless cantilever as described. Bead-modified cantilever were coated with Col I as described [29]. Measurements were performed in media (MEM supplemented with 5% FCS and 25 mM Hepes) at 37°C. For measurement of the mechanical maturation of FA, a bead-modified, functionalized and calibrated cantilever was lowered onto the margin of a single cell until a contact force of 1 nN was reached and was incubated in constant height mode for 2 minutes to ensure proper binding of the functionalized bead to the cell (**Fig. S3B**). Then, the bead-modified cantilever was repeatedly oscillated with amplitude of 200 nm and a frequency of 0.25 Hz for 20 minutes. During each oscillation cycle, a F–D curve was recorded. The maximum force of the retract F–D curve was extracted using the AFM data processing software (JPK Instruments). A relatively high variability

in initial forces resisting the cantilever retraction (1–4 nN) were observed and thus the retract force of each cycle was normalized against the value of the first cycle. The normalized values from each analyzed cell were then averaged for the different cell types.

### Immunofluorescence

For immunofluorescence analyses, cells on top of glass coverslips or PAA-gels were fixed with 4% PFA in PBS<sup>+</sup> for 10 min, washed with PBS<sup>+</sup> and subsequently blocked and permeabilized by 20 minutes incubations in 200 mM glycine in PBS and 0.5% BSA, 0.2% gelatin in PBS with 0.1% TX-100. Samples were incubated overnight in +4°C with the indicated primary antibodies, washed four times with the blocking solution and incubated for 1 hour at RT with secondary antibodies. Samples were washed with PBS and mounted on object glasses or, in the case of PAA-gel cultures, on top of larger cover glass using ImmMount<sup>TM</sup> (Thermo Scientific).

### Timelapse microscopy

Timelapse imaging was done using a CSUX1M 500, Yokokawa CSU-X1 spinning disk unit equipped with a Hamamatsu EM-CCD camera (512 $\times$ 512) and mounted on an Axio Observer Z1 (Zeiss) microscope using either 25X LD LCI Plan-Apochromat Multi-immersion (NA0.8, WD 0.57 mm) or 63X Plan-Apochromat Oil immersion (NA1.46, WD 0.1 mm) objectives at +37°C in a humidified stage-top CO<sub>2</sub>-incubator (PeCon GmbH). Alternatively, a TIRF-setup assembled on the same microscope frame was used in combination with the above-mentioned 63x objective and Hamamatsu ORCAII CCD-camera. For timelapse imaging, cells were trypsinized, washed once with PBS, resuspended into serum-free MEM and seeded onto glass-bottom culture dishes (Cellview<sup>TM</sup>, Greiner BioOne) that had been coated with 3  $\mu\text{g/ml}$  Col I, blocked using 1% BSA in PBS and washed twice with PBS and once with serum-free MEM prior to adding cell suspension.

### Cell culture on PAA gels

Cells were seeded onto collagen-coated polyacrylamide (PAA) gels of different elasticities. PAA gels were prepared with final concentration of acrylamide of 3 and 10% w/v from commercial 40% acrylamide/bisacrylamide solution (37.5:1) (Sigma). The gels contained 54 mM Hepes pH 7.0 and 1/2000 vol TEMED and 0.05% APS. 20  $\mu\text{l}$  or 40  $\mu\text{l}$  of PAA gels was applied on top of Surfacil (Pierce)-coated object glass and an activated coverslip was placed on top. Acid washed (incubated for 16 hours in 1 M HCl at 55°C, rinsed with water, washed with 70% EtOH prior to o/n incubation in 100% EtOH), dried and autoclaved coverslips were activated with 0.5% 3-aminopropyltrimethoxysilane (Sigma) in H<sub>2</sub>O, washed thrice with H<sub>2</sub>O, incubated with 0.5% glutaraldehyde in H<sub>2</sub>O, rinsed again with water and air-dried. PAA gels were let to polymerize for 8 minutes and washed with water. The gels were activated with 1 mg/ml NHS/Nitrophenyl Azide Crosslinker Sulfo-SANPAH (#22589, Thermo Scientific) in H<sub>2</sub>O by 15 minutes incubation under UV light followed by washing with 200 mM HEPES pH8.5. Col I (150  $\mu\text{g/ml}$ ) was added in 20 mM Hepes pH 8.5 and incubated o/n +4°C. ECM-linked gels were washed several times with PBS prior to experiments. Different acrylamide concentrations were tested and the experimental conditions were selected such that in stiff (10%) PAA gels most of the control cells spread efficiently whereas very little spreading of Itg $\alpha$ V-KD cells was observed. In the very soft (3%) PAA essentially none of the cells showed any significant degree of spreading.

## Immunoblotting

Cells were lysed either directly in 1xSDS sample buffer (for c-Src; 100 mM Tris-HCl, pH 8.8, 2.5 mM EDTA, 10% sucrose, 0.1% bromophenol blue, 10 mM dithiothreitol, and 1% SDS) or FAK lysis buffer (9.1 mM Na<sub>2</sub>HPO<sub>4</sub>, 1.7 mM NaH<sub>2</sub>PO<sub>4</sub> pH 7.2, 1% NP40, 0.25% sodium deoxycholate, 150 mM NaCl, 0.1% SDS, 1 mM EDTA) supplemented with protease (P8340 Sigma) and phosphatase (Sigma P5726) inhibitor cocktails. Proteins were separated using SDS-PAGE (Biorad) and transferred onto Protran nitrocellulose filters (Perkin-Elmer). Specific proteins were detected with indicated antibodies followed by chemiluminescence based on HRP-conjugated secondary antibodies (Pierce). Densitometric analysis was done using LAS-3000 imaging system (Fujifilm). The intensity ratios of activated (tyrosine-phosphorylated) FAK/c-Src to total FAK/c-Src were determined using Quantity One (Biorad). The ratio in control cells was set to 1 and the ratios from Itg $\beta$ 1-KD and Itg $\alpha$ V-KD cells are shown relative to that.

## Surface biotinylation and metabolic labeling of integrins

The high pH method was used [72].  $3 \times 10^6$  cells were plated onto collagen-coated and BSA-blocked  $\text{O}100$  mm dishes as described for washing assays. After 75 minutes, cells were washed once with PBS<sup>+</sup> and once with TEA-buffer (10 mM triethanolamine, 150 mM NaCl, 2 mM CaCl<sub>2</sub>, and 0.5 mM MgCl<sub>2</sub>, pH 9.0) followed by incubation with Sulfo-NHS-SS-biotin (0.5 mg/ml in TEA, #21331, Pierce) for 30 minutes on ice and washed twice with ice-cold PBS<sup>+</sup>. Cells were extracted with 0.5 ml of TNE-buffer (10 mM Tris-HCl pH 7.2, 2% Triton-X100, 150 mM NaCl, 1 mM EDTA) supplemented with protease and phosphatase inhibitor cocktail (#04693116001, Roche) and 10 mM glycine, scraped to microtubes, and inverted at 4°C for 30 minutes. Insoluble material was removed by centrifugation (15000 $\times$ g, 4°C 10 minutes). Protein concentration of the supernatant was determined with the bicinchoninic acid assay (23227, Pierce). 4xsample buffer was added and samples were heated at 95°C for 3 minutes. Biotinylated proteins were precipitated (o/n at 4°C) with 30  $\mu$ l of avidin-agarose beads (20219, Pierce) and released by heating (95°C, 3 minutes) in 30  $\mu$ l of 2xsample buffer. Samples were separated by SDS-PAGE and immunoblotted as described above.

Metabolic labeling was done as described previously with minor adjustments [61]. Cells were detached and washed twice with long term labeling medium containing 1/10<sup>th</sup> MEM and 9/10<sup>th</sup> DMEM without Methionine/Cysteine/L-glutamine (#D0422, Sigma), supplemented with 5% FBS, L-alanyl-L-glutamine (#A12860-01, Invitrogen) and 1% penicillin/streptomycin.  $4.4 \times 10^4$  cells per cm<sup>2</sup> were plated ( $\text{O}60$  mm dishes) in long term labeling medium containing 100  $\mu$ Ci of EXPRE<sup>35</sup>S<sup>35</sup>S Protein Labeling Mix (#NEG072, Perkin Elmer) and cultured for 18 hours. Radiolabeled cells were washed three times with ice-cold PBS<sup>+</sup> and extracted in 1 ml of RIPA-buffer (10 mM Tris-HCl pH 7.5, 0.5% SDS, 1% IGEPAL, 0.15 M NaCl, 1% Sodium deoxycholate + protease and phosphatase inhibitors; 4°C, 30 minutes). Insoluble material was removed by centrifugation (4°C, 10 minutes) and lysates were clarified by filtering through Ultrafree-CL centrifugal filter units (#UFC40HV00, Millipore). Protein concentration of the filtrate was determined with the bicinchoninic acid assay. Samples were incubated overnight with primary antibodies at 4°C and antigen-antibody complexes were recovered by adding 30  $\mu$ l of Protein A-Trisacryl (#20338, Pierce) and inverting for further 2 hours. Immunoprecipitates were pelleted (500 $\times$ g, 15 seconds) and washed thrice in RIPA-buffer and once with 10 mM Tris, pH 8.6. Trisacryl beads were

resuspended in 2xsample buffer and heated at 95°C for 3–5 minutes. The samples were then alkylated with iodoacetamide for 20 minutes at 37°C and fractionated by SDS-PAGE. Gels were fixed, impregnated with EN3HANCE (Perkin Elmer), dried and exposed to KODAK Biomax XAR film (#1651454001EA, Perkin Elmer).

## Supporting Information

**Figure S1 Analysis of integrin protein expression in the different integrin-KD cell lines.** **A)** The indicated amounts of control and Itg $\alpha$ V-KD#1 and #2 MDCK cell lysates were loaded for SDS-PAGE followed by detection of  $\alpha$ V-integrins by western blotting with rabbit anti- $\alpha$ V-integrin antibodies.  $\beta$ -actin was blotted as a loading control. **B)** Control MDCK and two independent Itg $\alpha$ V-KD cell lines were grown for 18 hours on  $\text{O}60$  mm TC-plastic dishes and metabolically labeled for 18 hours with <sup>35</sup>S-Methionine/Cysteine.  $\alpha$ V-integrins were immunoprecipitated with rabbit polyclonal anti- $\alpha$ V-integrin antibodies as described in materials and methods. **C)** Control and Itg $\beta$ 1-KD#2 MDCK cell lines were grown and metabolically labeled as in B) followed by immunoprecipitation of  $\beta$ 1-integrins using rabbit polyclonal anti  $\beta$ 1-integrin antibodies. The identity of the protein bands was confirmed with a series of metabolic labeling experiments using Itg $\alpha$ 2- (Fig. S1G) and Itg $\alpha$ 3-KD (data not shown) cells in which the respective protein bands were significantly reduced. **D)** Twenty micrograms of control and two Itg $\beta$ 3-KD MDCK cell lysates were loaded for SDS-PAGE followed by detection with mouse monoclonal  $\alpha$ V $\beta$ 3-integrin antibodies. Only a faint band at  $\sim$ 95 kDa was observed in the control cell lysate but the intensity of this band was further reduced in Itg $\beta$ 3-KD#2 cells and it was undetectable in Itg $\beta$ 3-KD#1 cell lysates **E)** The indicated amounts of control and two independent Itg $\alpha$  $\beta$ 6-KD MDCK cell lysates were loaded for SDS-PAGE followed by detection of  $\beta$ 6-integrins by western blotting with rabbit anti- $\beta$ 6-integrin antibodies. The antibody recognized two bands ( $\sim$ 110 kDa and  $\sim$ 85 kDa) both of which appeared to be reduced in Itg $\beta$ 6-KD cell lines. The calculated molecular weight of canine  $\beta$ 6-integrin is 86 kDa. **F)** The indicated amounts of control and two independent Itg $\beta$ 5-KD MDCK cell lysates were loaded for SDS-PAGE followed by detection of  $\beta$ 5-integrins by western blotting with sheep anti- $\beta$ 5-integrin antibodies. The antibody recognized a band at  $\sim$ 100 kDa that was down-regulated in one of the two Itg $\beta$ 5-KD cell lysates. **G)**  $\alpha$ V-integrins do not regulate the composition of  $\beta$ 1-integrin heterodimers. Control, Itg $\alpha$ 2- and Itg $\alpha$ V-KD#2 MDCK cell lines were metabolically labeled and  $\beta$ 1-integrins precipitated as in C). The pattern of  $\beta$ 1-integrins precipitated from control and Itg $\alpha$ V-KD cells is essentially identical. **H)**  $\alpha$ V-integrins do not co-cluster with  $\beta$ 1-integrins on Col I substrate. MDCK cells stably transfected with  $\alpha$ V-integrin-RFP fusion protein were trypsinized and seeded onto FN (upper panel) or Col I (lower panel)-coated glass in the absence of serum and allowed to settle for 30 minutes. The cells were imaged using spinning disk confocal microscope and 63x oil-immersion objective. Localization of  $\alpha$ V-integrin-RFP at the basal membrane is shown. Only relatively low-expressing cells were found but most of them showed clear accumulation of  $\alpha$ V-integrin-RFP fusion protein into pericellular foci on FN whereas on Col I substrate only uniform basal staining was observed. (TIF)

**Figure S2  $\alpha$ V $\beta$ 6 integrin is the major adhesive FN receptor in MDCK cells.** *Cell adhesion analysis by cell washing assay:* Single cell suspensions of control and the indicated Itg-KD MDCK cells were allowed to settle for 90 minutes on **A)**

fibronectin-, **B**) basement membrane-extract (BME)-, **C**) collagen I- or **D**) laminin-511 (LN-511)-coated tissue culture wells. Non-adherent cells were washed away and remaining adherent cells were fixed, stained and quantified. Adhesion of control cells to each coating was set to 1 and adhesion of the different Itg-KD cells is shown relative to the control. Each Itg-KD sample represents data from 4–10 independent experiments (shRNA#1 constructs) or 2–5 experiments (shRNA#2). Each value is normalized to a control value within the experiment and shows the mean + standard deviation (SD). P-values <0.01 are signified by (\*) for constructs which were analyzed in at least 3 independent experiments. ND: not determined. (TIF)

**Figure S3 Schemes of the SCFS setups.** **A)** *Measuring cell adhesion to collagen I-coated supports:* The position of a laser beam (red line), that is reflected off the back of a calibrated AFM cantilever, on a photodiode (PD) measures the deflection of the cantilever and thus the force acting on the cantilever. A single cell is bound to an AFM cantilever *via* the lectin concanavalin A. It is lowered onto a collagen I-coated support until a contact force of  $\approx 2$  nN is recorded. After keeping the cell, at constant height, on the support for a preset contact time, it is retracted from the support until cell and substrate are completely separated. During the approach-retract cycle, the force acting on the cantilever is recorded and can be plotted in a force-distance (F–D) curve. During cantilever retraction, the maximum downward force acting on the cantilever is referred to as the maximum force needed to detach the cell from the substrate ( $F_D$ ). After the major detachment force peak, smaller unbinding events can be detected. The majority of these events correspond to the rupture of membrane nanotubes (tethers). Tethers (T) are characterized by long force plateaus of constant force. **B)** *Measuring mechanical maturation of FA using AFM:* Cells were allowed to grow for 12 hours on collagen I-coated petri dishes. A collagen I-coated bead, attached to the apex of a tipless AFM cantilever, is lowered onto the margin of an isolated cell until a force of 1 nN is applied. The bead is maintained at constant height for 2 minutes to facilitate strong binding between cell and bead. Subsequently the cell-attached bead is oscillated for 20 minutes with an amplitude of 200 nm and a frequency of 0.25 Hz. The oscillation curve at the bottom shows the oscillating piezo movement that oscillates the cantilever to which the bead is attached. During oscillation, the force acting on the cantilever is recorded and plotted in a force vs time curve (upper oscillation curve). The sections of the force-time curve that are recorded during upward movement of the cantilever are analyzed for maximum force difference, as displayed in the inset (upper oscillation curve). (TIF)

**Figure S4 Depletion of  $\alpha$ V-integrins in leads to a cell spreading defect in MK3 cells.** **A)** Control and Itg $\alpha$ V-KD MK3 cells were trypsinized, seeded onto Col I-coated coverslips and allowed to settle for 240 minutes. Cells were fixed and stained for actin (TRITC-Phalloidin, red) and nuclei (DAPI, blue). **B)** Quantitation of the data shows the mean cell spreading area

## References

1. Saez A, Ghibaud M, Buguin A, Silberzan P, Ladoux B (2007) Rigidity-driven growth and migration of epithelial cells on microstructured anisotropic substrates. *Proc Natl Acad Sci U S A* 104(20): 8281–8286.
2. Paszek MJ, Zahir N, Johnson KR, Lakins JN, Rozenberg GI, et al. (2005) Tensional homeostasis and the malignant phenotype. *Cancer Cell* 8(3): 241–254.
3. Lo CM, Wang HB, Dembo M, Wang YL (2000) Cell movement is guided by the rigidity of the substrate. *Biophys J* 79(1): 144–152.

( $\mu\text{m}^2/\text{cell}$ )+SD of 2 independent experiments performed in duplicates. For each experiment and coating condition  $\sim 60$ –150 cells from 10–30 frames were analyzed. P-values <0.01 are signified by (\*). (TIF)

**Table S1 Validation of integrin-KD constructs.** **A)** shRNA target sequences used in this study and their respective KD-efficiencies. **B)** Oligos used for quantitative real-time PCR. (DOC)

**Movie S1 Spreading dynamics of control, Itg $\beta$ 1- and Itg $\alpha$ V-KD MDCK cells seeded onto collagen I substrate.** Control, Itg $\beta$ 1- and Itg $\alpha$ V-KD MDCK cells stably expressing vinculin-GFP were trypsinized, seeded onto collagen I-coated glass-bottom tissue culture dishes and imaged with a spinning disk confocal microscope and 25x objective for indicated times. Note that some Itg $\beta$ 1-KD cells are moving on the substrate indicating poor adhesion whereas most of the Itg $\alpha$ V-KD cells appear immobilized despite their inability to spread properly. (AVI)

**Movie S2 Timelapse imaging of GFP-Tln1 fusion protein in control, Itg $\alpha$ V- and Itg $\beta$ 1-KD MDCK cells seeded onto collagen I substrate.** Control, Itg $\beta$ 1- and Itg $\alpha$ V-KD MDCK cells stably expressing talin-1-GFP were trypsinized, seeded onto collagen I-coated glass-bottom tissue culture dishes in serum-free cell culture medium, allowed to settle for 30–60 minutes and imaged for 4.5 hours with 3 minutes time intervals using TIRF-microscopy and a 63x oil-immersion objective. (AVI)

**Movie S3 Timelapse imaging of GFP-vinculin fusion protein in control, Itg $\alpha$ V- and Itg $\beta$ 1-KD MDCK cells seeded onto collagen I substrate.** Control, Itg $\beta$ 1- and Itg $\alpha$ V-KD MDCK cells stably expressing vinculin-GFP were trypsinized, seeded onto collagen I-coated glass-bottom tissue culture dishes in serum-free cell culture medium, allowed to settle for 30–60 minutes and imaged for 4.5 hours with 3 minutes time intervals using TIRF-microscopy and a 63x oil-immersion objective. (AVI)

## Acknowledgments

Jaana Träskelin and Riitta Jokela are acknowledged for expert technical assistance. Veli-Pekka Ronkainen from the BCO imaging core facility is acknowledged for help with TIRF-microscopy. Carsten Werner is acknowledged for providing instrumentation and working space for the measurement of mechanical maturation of FA. We thank Jyrki Heino and Johanna Myllyharju for critically reading the manuscript.

## Author Contributions

Conceived and designed the experiments: AM TT SM JF DM JM KM. Performed the experiments: TT SM JF NS AM. Analyzed the data: TT SM JF NS DM AM. Contributed reagents/materials/analysis tools: KM JM CW. Wrote the paper: AM TT JF DM.

7. Li S, Harrison D, Carbonetto S, Fassler R, Smyth N, et al. (2002) Matrix assembly, regulation, and survival functions of laminin and its receptors in embryonic stem cell differentiation. *J Cell Biol* 157(7): 1279–1290.
8. Butcher DT, Alliston T, Weaver VM (2008) A tense situation: Forcing tumour progression. *Nat Rev Cancer* 9(2): 108–122.
9. Levental KR, Yu H, Kass L, Lalkins JN, Egeblad M, et al. (2009) Matrix crosslinking forces tumor progression by enhancing integrin signaling. *Cell* 139(5): 891–906.
10. Mao Y, Schwarzbauer JE (2005) Fibronectin fibrillogenesis, a cell-mediated matrix assembly process. *Matrix Biol* 24(6): 389–399.
11. Velling T, Risteli J, Wennerberg K, Mosher DF, Johansson S (2002) Polymerization of type I and III collagens is dependent on fibronectin and enhanced by integrins alpha 1beta 1 and alpha 2beta 1. *J Biol Chem* 277(40): 37377–37381.
12. Kadler KE, Hill A, Canty-Laird EG (2008) Collagen fibrillogenesis: Fibronectin, integrins, and minor collagens as organizers and nucleators. *Curr Opin Cell Biol* 20(5): 495–501.
13. Raghavan S, Bauer C, Mundschaug G, Li Q, Fuchs E (2000) Conditional ablation of beta1 integrin in skin: severe defects in epidermal proliferation, basement membrane formation, and hair follicle invagination. *J Cell Biol* 150(5): 1149–1160.
14. Lohikangas L, Gullberg D, Johansson S (2001) Assembly of laminin polymers is dependent on beta1-integrins. *Exp Cell Res* 265(1): 135–144.
15. Roca-Cusachs P, Gauthier NC, Del Rio A, Sheetz MP (2009) Clustering of alpha(5)beta(1) integrins determines adhesion strength whereas alpha(v)beta(3) and talin enable mechanotransduction. *Proc Natl Acad Sci U S A* 106(38): 16245–16250.
16. Abair TD, Sundaramoorthy M, Chen D, Heino J, Ivaska J, et al. (2008) Crosstalk between integrins alpha1beta1 and alpha2beta1 in renal epithelial cells. *Exp Cell Res* 314(19): 3593–3604.
17. White DP, Caswell PT, Norman JC (2007) Alpha v beta3 and alpha5beta1 integrin recycling pathways dictate downstream rho kinase signaling to regulate persistent cell migration. *J Cell Biol* 177(3): 515–525.
18. Blystone SD, Slater SE, Williams MP, Crow MT, Brown EJ (1999) A molecular mechanism of integrin crosstalk: Alphavbeta3 suppression of calcium/calmodulin-dependent protein kinase II regulates alpha5beta1 function. *J Cell Biol* 145(4): 889–897.
19. Retta SF, Cassara G, D'Amato M, Alessandro R, Pellegrino M, et al. (2001) Cross talk between beta(1) and alpha(V) integrins: Beta(1) affects beta(3) mRNA stability. *Mol Biol Cell* 12(10): 3126–3138.
20. Howlett AR, Bailey N, Damsky C, Petersen OW, Bissell MJ (1995) Cellular growth and survival are mediated by beta 1 integrins in normal human breast epithelium but not in breast carcinoma. *J Cell Sci* 108: 1945–1957.
21. Ruoslahti E (1996) RGD and other recognition sequences for integrins. *Annu Rev Cell Dev Biol* 12: 697–715.
22. Leiss M, Beckmann K, Giros A, Costell M, Fassler R (2008) The role of integrin binding sites in fibronectin matrix assembly in vivo. *Curr Opin Cell Biol* 20(5): 502–507.
23. Wierzbicka-Patynowski I, Schwarzbauer JE (2003) The ins and outs of fibronectin matrix assembly. *J Cell Sci* 116: 3269–3276.
24. Matlin KS, Haus B, Zuk A (2003) Integrins in epithelial cell polarity: Using antibodies to analyze adhesive function and morphogenesis. *Methods* 30(3): 235–246.
25. Pierschbacher MD, Ruoslahti E (1984) Cell attachment activity of fibronectin can be duplicated by small synthetic fragments of the molecule. *Nature* 309(5963): 30–33.
26. Aumailley M, Gerl M, Sonnenberg A, Deutzmann R, Timpl R (1990) Identification of the arg-gly-asp sequence in laminin A chain as a latent cell-binding site being exposed in fragment P1. *FEBS Lett* 262(1): 82–86.
27. Busk M, Pytela R, Sheppard D (1992) Characterization of the integrin alpha v beta 6 as a fibronectin-binding protein. *J Biol Chem* 267(9): 5790–5796.
28. Montgomery AM, Reisfeld RA, Chersesh DA (1994) Integrin alpha v beta 3 rescues melanoma cells from apoptosis in three-dimensional dermal collagen. *Proc Natl Acad Sci U S A* 91(19): 8856–8860.
29. Friedrichs J, Helenius J, Muller DJ (2010) Quantifying cellular adhesion to extracellular matrix components by single-cell force spectroscopy. *Nat Protoc* 5(7): 1353–1361.
30. Helenius J, Heisenberg CP, Gaub HE, Muller DJ (2008) Single-cell force spectroscopy. *J Cell Sci* 121: 1785–1791.
31. Krieg M, Helenius J, Heisenberg CP, Muller DJ (2008) A bond for a lifetime: Employing membrane nanotubes from living cells to determine receptor-ligand kinetics. *Angew Chem Int Ed Engl* 47(50): 9775–9777.
32. Friedrichs J, Manninen A, Muller DJ, Helenius J (2008) Galectin-3 regulates integrin alpha 2beta 1-mediated adhesion to collagen-I and -IV. *J Biol Chem* 283: 32264–32272.
33. Friedrichs J, Torkko JM, Helenius J, Teravainen TP, Fullekrug J, et al. (2007) Contributions of galectin-3 and -9 to epithelial cell adhesion analysed by single cell force spectroscopy. *J Biol Chem* 282(40): 29375–29383.
34. Geiger B, Spatz JP, Bershadsky AD (2009) Environmental sensing through focal adhesions. *Nat Rev Mol Cell Biol* 10(1): 21–33.
35. Schwarz DS, Ding H, Kennington L, Moore JT, Schelter J, et al. (2006) Designing siRNA that distinguishes between genes that differ by a single nucleotide. *PLoS Genet* 2(9): e140.
36. Humphries JD, Wang P, Streuli C, Geiger B, Humphries MJ, et al. (2007) Vinculin controls focal adhesion formation by direct interactions with talin and actin. *J Cell Biol* 179(5): 1043–1057.
37. Mak GZ, Kavanaugh GM, Buschmann MM, Stickley SM, Koch M, et al. (2006) Regulated synthesis and functions of laminin 5 in polarized madin-darby canine kidney epithelial cells. *Mol Biol Cell* 17: 3664–3677.
38. Zaidel-Bar R, Cohen M, Addadi L, Geiger B (2004) Hierarchical assembly of cell-matrix adhesion complexes. *Biochem Soc Trans* 32: 416–420.
39. Hirata H, Tatsumi H, Sokabe M (2008) Mechanical forces facilitate actin polymerization at focal adhesions in a zyxin-dependent manner. *J Cell Sci* 121: 2795–2804.
40. Yoshigi M, Hoffman LM, Jensen CC, Yost HJ, Beckerle MC (2005) Mechanical force mobilizes zyxin from focal adhesions to actin filaments and regulates cytoskeletal reinforcement. *J Cell Biol* 171(2): 209–215.
41. Stanchi F, Grashoff C, Nguemni Yonga CF, Grall D, Fassler R, et al. (2009) Molecular dissection of the ILK-PINCH-parvin triad reveals a fundamental role for the ILK kinase domain in the late stages of focal-adhesion maturation. *J Cell Sci* 122: 1800–1811.
42. Zervas CG, Gregory SL, Brown NH (2001) Drosophila integrin-linked kinase is required at sites of integrin adhesion to link the cytoskeleton to the plasma membrane. *J Cell Biol* 152(5): 1007–1018.
43. Zhang Y, Chen K, Tu Y, Velyvis A, Yang Y, et al. (2002) Assembly of the PINCH-ILK-CH-ILKBP complex precedes and is essential for localization of each component to cell-matrix adhesion sites. *J Cell Sci* 115: 4777–4786.
44. Kornberg L, Earp HS, Parsons JT, Schaller M, Juliano RL (1992) Cell adhesion or integrin clustering increases phosphorylation of a focal adhesion-associated tyrosine kinase. *J Biol Chem* 267(33): 23439–23442.
45. Hannigan GE, Leung-Hagstjejn C, Fitz-Gibbon L, Coppolino MG, Radeva G, et al. (1996) Regulation of cell adhesion and anchorage-dependent growth by a new beta 1-integrin-linked protein kinase. *Nature* 379: 91–96.
46. Wu C, Dedhar S (2001) Integrin-linked kinase (ILK) and its interactors: A new paradigm for the coupling of extracellular matrix to actin cytoskeleton and signaling complexes. *J Cell Biol* 155: 505–510.
47. Eide BL, Turck CW, Escobedo JA (1995) Identification of tyr-397 as the primary site of tyrosine phosphorylation and pp60src association in the focal adhesion kinase, pp125FAK. *Mol Cell Biol* 15(5): 2819–2827.
48. Mitra SK, Schlaepfer DD (2006) Integrin-regulated FAK-src signaling in normal and cancer cells. *Curr Opin Cell Biol* 18(5): 516–523.
49. Reinhart-King CA, Dembo M, Hammer DA (2003) Endothelial cell traction forces on RGD-derivatized polyacrylamide substrata. *Langmuir* 19: 1573–1579.
50. Solon J, Levental I, Sengupta K, Georges PC, Jamney PA (2007) Fibroblast adaptation and stiffness matching to soft elastic substrates. *Biophys J* 93(12): 4453–4461.
51. Davis GE (1992) Affinity of integrins for damaged extracellular matrix: Alpha v beta 3 binds to denatured collagen type I through RGD sites. *Biochem Biophys Res Commun* 182(3): 1025–1031.
52. Caswell PT, Chan M, Lindsay AJ, McCaffrey MW, Boettiger D, et al. (2008) Rab-coupling protein coordinates recycling of alpha5beta1 integrin and EGFR1 to promote cell migration in 3D microenvironments. *J Cell Biol* 183(1): 143–155.
53. Grundstrom G, Mosher DF, Sakai T, Rubin K (2003) Integrin alphavbeta3 mediates platelet-derived growth factor-BB-stimulated collagen gel contraction in cells expressing signaling deficient integrin alpha2beta1. *Exp Cell Res* 291(2): 463–473.
54. Cooke ME, Sakai T, Mosher DF (2000) Contraction of collagen matrices mediated by alpha2beta1A and alpha(v)beta3 integrins. *J Cell Sci* 113: 2375–2383.
55. Wang P, Ballestrem C, Streuli CH (2011) The C terminus of talin links integrins to cell cycle progression. *J Cell Biol* 195(3): 499–513.
56. Calderwood DA, Zent R, Grant R, Rees DJ, Hynes RO, et al. (1999) The talin head domain binds to integrin beta subunit cytoplasmic tails and regulates integrin activation. *J Biol Chem* 274(40): 28071–28074.
57. Tadokoro S, Shattil SJ, Eto K, Tai V, Liddington RC, et al. (2003) Talin binding to integrin beta tails: A final common step in integrin activation. *Science* 302(5642): 103–106.
58. Zhang X, Jiang G, Cai Y, Monkley SJ, Critchley DR, et al. (2008) Talin depletion reveals independence of initial cell spreading from integrin activation and traction. *Nat Cell Biol* 10: 1062–1068.
59. Hall DE, Reichardt LF, Crowley E, Holley B, Moezzi H, et al. (1990) The alpha 1/beta 1 and alpha 6/beta 1 integrin heterodimers mediate cell attachment to distinct sites on laminin. *J Cell Biol* 110(6): 2175–2184.
60. Takada Y, Puzon W (1993) Identification of a regulatory region of integrin beta 1 subunit using activating and inhibiting antibodies. *J Biol Chem* 268(23): 17597–17601.
61. Schoenenberger CA, Zuk A, Zinkl GM, Kendall D, Matlin KS (1994) Integrin expression and localization in normal MDCK cells and transformed MDCK cells lacking apical polarity. *J Cell Sci* 107: 527–541.
62. Chen FA, Repasky EA, Bankert RB (1991) Human lung tumor-associated antigen identified as an extracellular matrix adhesion molecule. *J Exp Med* 173(5): 1111–1119.
63. Ferletta M, Ekblom P (1999) Identification of laminin-10/11 as a strong cell adhesive complex for a normal and a malignant human epithelial cell line. *J Cell Sci* 112: 1–10.

64. Valerius MT, Patterson LT, Witte DP, Potter SS (2002) Microarray analysis of novel cell lines representing two stages of metanephric mesenchyme differentiation. *Mech Dev* 112(1–2): 219–232.
65. Schuck S, Manninen A, Honsho M, Fullekrug J, Simons K (2004) Generation of single and double knockdowns in polarized epithelial cells by retrovirus-mediated RNA interference. *Proc Natl Acad Sci U S A* 101(14): 4912–4917.
66. Franco SJ, Rodgers MA, Perrin BJ, Han J, Bennin DA, et al. (2004) Calpain-mediated proteolysis of talin regulates adhesion dynamics. *Nat Cell Biol* 6(10): 977–983.
67. Pietila R, Natynki M, Tammela T, Kangas J, Pulkki KH, et al. (2012) Ligand oligomerization state controls Tie2 receptor trafficking and angiopoietin-2-specific responses. *J Cell Sci* 125: 2212–2223.
68. Rasband WS (1997–2010) ImageJ, *U. S. national institutes of health*, Bethesda, MD, USA.
69. Meijering E, Dzyubachyk O, Smal I (2012) Methods for cell and particle tracking. *Methods Enzymol* 504: 183–200.
70. Hutter JL, Bechhoefer J (1993) Calibration of atomic-force microscope tips. *Rev Sci Instrum* 64(7): 1868–1873.
71. Krieg M, Arboleda-Estudillo Y, Puech PH, Kafer J, Graner F, et al. (2008) Tensile forces govern germ-layer organization in zebrafish. *Nat Cell Biol* 10(4): 429–436.
72. Gottardi CJ, Dunbar LA, Caplan MJ (1995) Biotinylation and assessment of membrane polarity: Caveats and methodological concerns. *Am J Physiol* 268: F285–F295.